

A real-time hourly water index for flood risk monitoring: Pilot studies in Brisbane, Australia, and Dobong Observatory, South Korea


Ravinesh C. Deo  · Hi-Ryong Byun · Ga-Byn Kim · Jan F. Adamowski

Received: 25 December 2016 / Accepted: 15 June 2018 / Published online: 4 July 2018
© Springer International Publishing AG, part of Springer Nature 2018

Abstract A water resources index based on weight-accumulated precipitation over the passage of time in heavy rainfall events is used in this study for monitoring flood risk and peak danger, as well as to develop flood warnings. In this research, an hourly water resources index (WRI_{hr}) based on rainfall accumulations over the passage of time is proposed. WRI_{hr} is able to monitor flood risk by taking into account the hourly effective precipitation that accumulates the precipitation (P_{hr}) of both current and antecedent hours, while the contributions from the preceding hours is subjected to a time-dependent reduction function that addresses the depletion of water volume by various hydrological processes (e.g., discharge, runoff, evapotranspiration). By converting rainfall into a water resources index (WRI), the hourly precipitation over a 24-h period is

redistributed to formulate a long-term water resources index (WRI_{hr-L}) that monitors flood status based on long-term (more than 1 year) fluctuations in P_{hr} and a short-term water resources index (WRI_{D-hr-S}) that considers shorter ($D = 24\text{--}148$ hourly) accumulations of the P_{hr} data. WRI was assessed for its potential in flood monitoring at two hydrologically diverse sites: Dobong (South Korea; August 1998) and Brisbane (Australia; December 2010–January 2011), and its applicability was verified using river water level (H) measurements at hydrological stations. The power spectrum density and spectral coherence of hourly rainfall, river water level, and the corresponding WRI showed good agreements, as did the low and high frequency wavelet components using the discrete wavelet transform algorithm. Importantly, $WRI_{24-hr-S}$ computed over 24 hourly accumulation periods was able to mimic the risk of short-term (flash-style) floods caused by concentrated rainfall, whereas WRI_{hr-L} was more useful for flood risk assessment caused by an event over a long-term period. Dynamical changes in H were closely in-phase with the patterns of change noted in the WRI_{hr} over the respective temporal scale. We conclude that the proposed WRI was able to replicate the flood evolution over the passage of time and, therefore, could possibly aid in the early warning of water-related disasters, demonstrating its practicality for continuous monitoring of the flood risk when a sustained period of rainfall event is observed.

R. C. Deo 
School of Agricultural, Computational and Environmental Sciences, Center for Applied Climate Sciences, Institute of Agriculture and Environment, University of Southern Queensland, Springfield Campus, Springfield, QLD 4300, Australia
e-mail: ravinesh.deo@usq.edu.au

H.-R. Byun  · G.-B. Kim
Departments of Environmental and Atmospheric Sciences, Pukyong National University, Yongsoro-45, Nam-Gu, Busan 48513, Republic of Korea
e-mail: windbig@hanmail.net

J. F. Adamowski
Department of Bioresource Engineering, Faculty of Agricultural & Environmental Sciences, McGill University, Montreal, Québec H9X 3V9, Canada

Keywords Hourly water resources index · Short- and long-term flood monitoring · Korea · Australia · Antecedent rainfall · Flood monitoring system

Nomenclature

<i>API</i>	Anterior Precipitation Index
<i>D</i>	Summation period (e.g., 24, 48, 72... 365)
<i>H</i>	River height (m)
<i>m</i>	Timescale (days)
P_{hr}	Hourly raw rainfall
P_m	Daily raw rainfall
P_E	Daily effective rainfall
P_{max}	Maximum monthly precipitation
$P_{hr,t}$	Hourly raw rainfall (t = the specific time, e.g., 1, 2, ..., 24 h)
P_{E-hr}	Hourly effective rainfall
Q_{DR}	River discharge rate ($m^3 s^{-1}$)
<i>SPI</i>	Standardized Precipitation Index
<i>t</i>	Timescale (hours)
<i>W</i>	Weighting factor
<i>WRI</i>	Water Resources Index
$WRI_{148-hr-S}$	148 hourly <i>WRI</i>
$WRI_{24-hr-S}$	24 hourly <i>WRI</i>
$WRI_{48-hr-S}$	48 hourly <i>WRI</i>
$WRI_{72-hr-S}$	72 hourly <i>WRI</i>
$WRI_{96-hr-S}$	96 hourly <i>WRI</i>
WRI_{hr}	Hourly Water Resources Index
WRI_{hr-L}	Long-term hourly Water Resources Index
WRI_{hr-S}	Short-term hourly Water Resources Index
Subscript “S”	Short-term (nominally 24, 48, 72, and 96 hourly)
Subscript “L”	Long-term (nominally 365 days or more)
Subscript “24”	24 hourly
	All units are in mm unless stated otherwise.

Introduction

Global climate models are important for large-scale climate projections but they often have challenges in simulating localized and timely concentration of rainwater volume that can cause a flood hazard due to high-intensity rainfall occurring at random or short-duration intervals. Statistical metrics that explore trends in monthly rainfall (e.g., Seiler et al. 2002) and daily indices (e.g., Deo et al. 2015; Lu 2009; Nosrati et al.

2011) do not adequately represent the risk caused by short-duration events (IPCC 2001). For a local assessment of a flood hazard, the probability of an event is intrinsically dependent on the rain intensity and its accumulation in a sizable volume of water. However, flood risk is moderated by redistribution of this rainwater over the passage of time due to many hydrological factors such as suction, seepage, drainage discharge, topography and evapotranspiration, infiltration, and percolation (Lu 2009; Ma et al. 2014). Due to the difficulty of measuring any of these parameters, especially over a short-term period and the stochastic nature of a rainfall event, a simple and robust method that is able to monitor the progression of a flood event is a useful tool for flood risk management.

Many parts of South Korea and Australia experience intense flooding. In Korea, the risk is high in the typhoon season (Ghosh et al. 2015; HRFCO 2014; Moon and Kim 2015), while in Australia, a La Nina event is associated with floods largely in eastern Queensland and New South Wales (Keogh et al. 2011; Seqwater 2011). South Korean floods result in an annual loss of approximately \$US1.2 billion (Ghosh et al. 2015). For example, the July 2011 Seoul flood killed 49 people and left more than 77 dead or missing. At least 86 power outages were recorded following landslides that affected 125,000 people with 11,000 Koreans forced to evacuate. Similarly, in Australia, almost 93% of all damages to buildings from 1900 to 2003 were attributable to cyclones and floods (Crompton 2011). From 1971 to 2003, floods accounted for about 29% of all natural disasters, with a total cost of \$US240 million (BTRE 2002). In particular, the December 2010–January 2011 flood event, which is used as a case study in this paper, was highly catastrophic, and resulted in more than 56,000 insurance payouts worth \$US2.00 billion (Box et al. 2013; van den Honert and McAneney 2011). Studies of flood behavior over short-term periods requires novel methods that can monitor the flood progression over the passage of time and that can be used to help inform the public of an upcoming flood event.

In Australia and Korea, flood monitoring is undertaken in conjunction with weather forecasts to provide an advanced warning or seasonal forecasts of a heightened chance of a flood in the upcoming months. In both nations, an estimation of river heights, streamflow, time of rainfall occurrence, and peak flow rates at a specified point in time resulting from changes in rainfall are carried out continuously. The Australian Bureau of

Meteorology, in partnership with agencies at state and local government levels, provides water level forecasts in rivers at critical locations. Local governments and emergency agencies interpret the river water level forecasts and provide advice on floods. Approaches such as radar and satellite images are used for tracking heavy rain movement, and generally rainfall in the next 1 to 4 h are forecasted based on the images in combination with computer models. Despite their overall effectiveness, these methods are time-consuming, expensive, and complex to implement in geographically diverse locations (Inquiry 2011; NCC 2011; Seqwater 2011; Yeo 2002).

In Korea, now-casting systems for floods are in place where these inter-connected monitoring systems warn against disasters. They comprise the Cell Broadcasting Service mobile phone message system, automatic verbal notification system, automatic rainfall warning system, disaster notification board system, TV disaster warning broadcasting systems, and the radio disaster warning broadcasting system (Ghosh et al. 2015; HRFCO 2014; Lee and Hur 2000; Park 2006). In addition, alternative flood warning systems are being explored in Korea. For example, one new approach involves an urban flood warning system that predicts flash rain by radar and satellite images to rapidly predict inland flooded areas for rapid decision-making (Moon and Kim 2015). While these systems are also effective, they are expensive. As such, there is a need for affordable approaches to continuously monitor flood events (e.g., Deo et al. 2015; Georgakakos 2006; Nosrati et al. 2011) to help design flood warning systems.

Development of a flood system over hourly periods has been explored by researchers. Beck et al. (2015) noted that rainfall events exhibit spatio-temporal variability in early morning and afternoon, and therefore, daily average data is inappropriate for risk detection. Helloco et al. (2003) tested a satellite system for flash floods in Garonne sub-basins using hourly rainfall radar images. Flash Flood Guidance is used to provide global-scale flood monitoring using hourly to six hourly rainfall data for streams that range in size from 25 to 200 km² (Hill et al. 2010). The NWS River Forecast system, based on the Sacramento Model (Burnash and Singh 1995), is a standard flood model in the USA while in Australia, RORB (Laurenson et al. 1995) is employed. A new warning system (“Hydrological Flood Intelligence,” HyFI) was developed by the Australian Bureau of Meteorology that collects rainfall and river

data from 3000 river and 3500 gauge sites on an hourly basis, coupled with statistical and modeling tools applied to construct a warning system (Jayasuriya et al. 2011). Although HyFI is a reliable system, it is not very flexible, and it does not support new hydrological models and forecasting tools or improved rainfall products (BOM 2012). Moreover hydrological models incorporate physical (i.e., rainfall runoff) equations that are approximations of reality; hence, the output may not be able to exactly predict the risk of a flood event at an operational level (Jonsdottir et al. 2006).

In general, flood disasters are dependent on several characteristics (e.g., peak rainfall intensity, rainfall event duration) (Gaál et al. 2014). In order to monitor a flood risk during and after a rain event, a statistical method that utilizes hydrologically relevant data is an a priori stratagem. As flood impacts are of a quantitative nature by virtue of their dependence on accumulated water volume, the timing and rainfall amount is proportional to risk (Doswell et al. 1996). A metric should monitor the magnitude of rainfall changes and subsequent flood extent based on how the water volume dissipates over time (Deo et al. 2015). Ideally, it should assess progressive water accumulations that can trigger a flood within and after a heavy rain period, and more importantly, it must operate over short-term (e.g., hourly) periods, in order to identify the subtle changes in risk (Lu 2009, 2012; Lu et al. 2013).

In a recent study (Deo et al. 2015) which followed earlier work by the authors of this paper (Byun and Jung 1998; Byun and Lee 2002; Choi et al. 2012; Lu 2009; Nosrati et al. 2011), a flood index based on daily effective precipitation (P_E) was found to be useful for flood monitoring in Queensland. P_E was a weighted sum of current and antecedent rainfall, and a time-dependent reduction formula was applied on the recent (vs. older) rainfall to account for water accumulation due to hydrological factors (An and Kim 1998; Lee 1998). This index exhibited a peak in a flood period that corresponded to a rise in the Available Water Resources Index (AWRI) (Byun and Lee 2002), and a change in its magnitude was in-phase with river water levels for the Brisbane flood in December 2010–January 2011. Although this index was verified for flood assessment, it was restricted to a daily time step. However, for a short period, high-intensity event which triggers a rapid response (e.g., flash flood), an hourly water resources index is a better measure of the flood risk (Chen et al. 2015).

The novelty of this paper is to advance the concept of flood monitoring with the *AWRI* (e.g., (Byun and Jung 1998; Lu 2009; Lu et al. 2015; Nosrati et al. 2011) and formulate a new Water Resources Index (*WRI*) for hourly monitoring of a flood event considering rainfall accumulation redistributed by an objective formula factored viz a time-dependent function. With an overall purpose to validate the robustness of the proposed method for hydrologically diverse contexts, the specific aims of this paper are fourfold: (1) to develop an easy-to-interpret, hourly-based *WRI* (WRI_{hr}) that allows for continuous flood risk monitoring; (2) to construct a short-term water resources index ($WRI_{24-hr-S}$) with rainfall accumulation over a daily (i.e., 24 hours) to weekly (i.e., 7 days or 168 h) period; (3) to construct a long-term water resources index (WRI_{hr-L}) with hourly rainfall accumulations over a precipitation cycle (365 days) considering current and antecedent (redistributed) rainfall; and (4) to verify the robustness of WRI_{hr-S} for short-term (flash flood) application using dam outflow data and WRI_{hr-L} for large-scale flooding situations, inundations, or evacuation warning using river water heights. To accomplish this, case studies were explored at vulnerable sites in Brisbane, Australia, and Dobong Observatory, South Korea, which have experienced chronic and catastrophic flooding (Box et al. 2013; Deo et al. 2015; Inquiry 2011; Khan et al. 2014; O'Brien 2011). In addition, records of water disasters (e.g., inundations, landslides, evacuations) were collated from newspapers and government and non-government agencies to verify the ability of *WRI* to indicate damages due to a flood event.

Materials and methods

Study area and hydrological data

In accordance with previous research (Box et al. 2013; Deo et al. 2015; Inquiry 2011; Khan et al. 2014; O'Brien 2011), flood-prone zone sites in our case study include Dobong Observatory, South Korea (WMO ID 47406, 43.56° N, 141.37° E) and the Brisbane River, Queensland (BOM ID 143007A; 26.80° S; 152.28° E). We purposely selected two study sites (in two different countries) that exhibit unique different hydrological characteristics and, therefore, provide a robust assessment of the proposed flood monitoring index. Dobong is located in the outskirts of Seoul within an urban branch of the Han River that experiences significant flooding

events (HRFCO 2014; Lee and Hur 2000; Moon and Kim 2015), while the Brisbane River (the longest river in southeast Queensland) which merges with Stanley River downstream of Somerset Dam, is in Lockyer Valley, which experienced Australia's worst flood (Box et al. 2013; van den Honert and McAneney 2011) (Fig. 1).

Data consists of hourly precipitation (P_{hr}) from 01 January 1998 to 31 December 2013 for Dobong Observatory, acquired from the Han River Flood Control Office (HRFCO 2014) and 01 January 2008 to 31 December 2013 for the Brisbane River, acquired from the Queensland Water Monitoring Data Portal, Department of Environment and Resource Management (DNRM 2014). It is important to clarify that these data are for the most intense rainfall periods. For example, for Australia, the data were taken from a period where intense floods were experienced during the November 2010 to January 2011 flood events, as used in previous studies (Deo et al. 2015). In addition to the P_{hr} data, the secondary data applied for validation purposes were based on average river heights (H) for each hourly period. For Dobong Observatory, H were acquired for Jungryang Stream (approximately 9.2 km from the site) while for Brisbane, H were available at the river site where P_{hr} were recorded. The period over which data were available covered the catastrophic flood events at both locations (including the August 1998 event for Dobong and the December 2010–January 2011 event for Brisbane).

In order to also examine the link between *WRI* and water-related disasters, anecdotal records of flood dates and extents of inundation, landslides, evacuations, etc., for the August 1998 event in Dobong Observatory site were acquired. The records acquired from online and printed newspaper sources and reports and magazine articles (HRFCO 2014; Lee and Hur 2000; MOLIT 1999, 2014; Yonhapnews 1998) provide information on the estimated time of disasters. It is important to note that only major water-related disasters in the August 1998 flood event in Seoul are considered for comparison with the hourly *WRIs*, as an exhaustive list of all (major as well as minor events) damages is difficult to collate.

In terms of hydrological statistics (Table 1), the mean, minimum, and maximum annual precipitation at Dobong Observatory is twofold larger than Brisbane, and the standard deviation is 9% higher. Although the difference in mean and minimum river height (H) for the sites are similar, the maximum H value at Brisbane is \approx

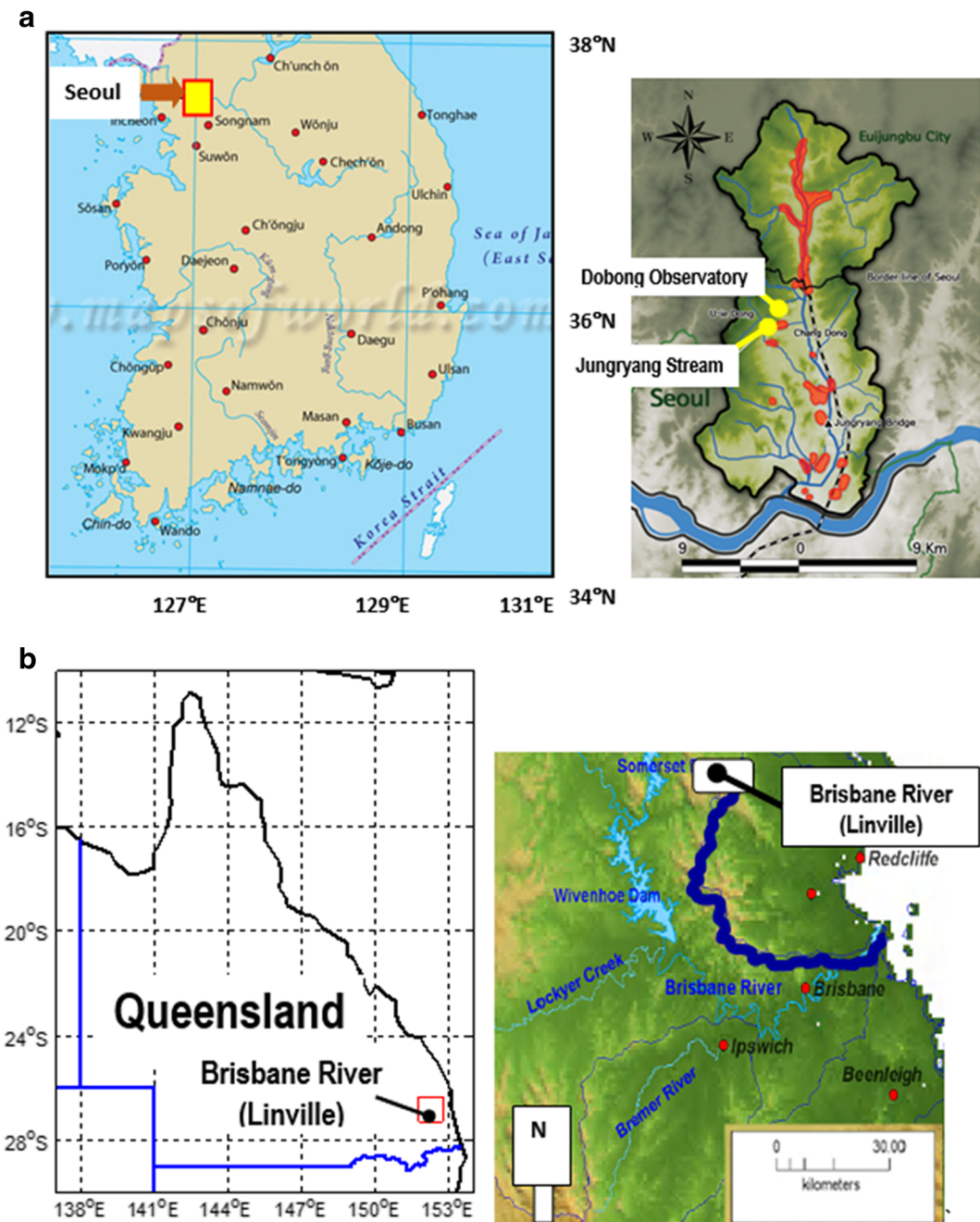


Fig. 1 **a** Map of Seoul, Korea (left) with inundated areas (red) near Jungryang Stream (blue) and nearby topography (right) (Lee and Hur 2000). The thicker blue line shows Han River and Eastern Trunk Road and dotted shows the Eastern Trunk Road (inundated

August 1998). **b** Map of Queensland, Australia (left) with Brisbane River (Linville) site (middle) and its topography (right). The thick blue line shows the river from the study site to the river's major inlet (Deo et al. 2015; van den Honert and McAneney 2011)

40% larger than the maximum H recorded at Dobong Observatory for the two flood cases considered. It is noteworthy that the maximum H occurred at 05:00 am LST (11 January 2011) for the Brisbane site and at

07:00 am LST (06 August 1998) for the Jungryang Bridge. In terms of monthly climatology (Fig. 2), an opposite trend is noted for the two sites where the summer (December–January) period is extremely wet

(for Brisbane), but the winter (July–August) period is dry. In contrast, for Dobong Observatory, most of the recorded rainfall is concentrated from July–August, but the maximum hourly water level is recorded in the August 1998 flood event. In summary, the diverse hydrological conditions recorded for the two study sites are thus useful for testing the versatility of the proposed WRI_{hr} for flood monitoring.

Physical rationale

In this study, we assume that the variation of flood extent can be understood in the way that the flood progression is assessed by monitoring the changes in accumulated volume of water resources¹ over the passage of time as a result of, and during, a series of heavy rain events (Deo et al. 2015; Godt et al. 2006; Lu 2009; Yu et al. 2006). The task of accurately measuring rainfall distribution, infiltration and individual factors (e.g., runoff or evapotranspiration) that acts to moderate the depletion of water in geographically diverse study sites is difficult (Sassa and Canuti 2008). However, rainfall data from a measurement gauge, which can be easily acquired, and which can be used to examine the flood risk based on a statistical formula, is an ideal parameter for flood assessment. Consequently, statistical relationships between changes in precipitation, river and streamflow discharge used in rainfall–runoff models have been used to quantify the effect of antecedent soil-water content on flood risk in a period preceding the heavy rainfall event. Following earlier work on daily and monthly flood monitoring (Deo et al. 2015; Du et al. 2013; Lu 2009; Nosrati et al. 2011; Seiler et al. 2002), this study develops an hourly water resources index (WRI_{hr}) to allow for continuous monitoring of flood risk.

In general, any form of WRI should utilize the logic that the risk of a flood will rely not only on the current but also on the pre-existing rainfall, over a spatio-temporal domain. Therefore, the concept of “effective” precipitation (P_{E-hr}) which in this work has been adopted from earlier papers (Deo et al. 2015; Nosrati et al. 2011) was similar to the “weighted average precipitation” proposed for daily flood monitoring (Lu 2009). In this study, the WRI_{hr} was formulated by

superposition of the current day’s hourly single input rainfall (P) onto an antecedent hour’s P . The conversion of hourly P into accumulated volume of water was governed by a time-dependent reduction function (e.g., (Deo et al. 2015; Lu 2009).

Denoting P_m = daily rainfall where m ($1 \leq m \leq 365$ days), and N is the duration of the summation of the antecedent (or preceding) period (nominally 365 days for the usual hydrological cycle), then P_E for the current (i th) day can be written as (Byun and Lee 2002; Deo et al. 2015):

$$P_{E_i} = \sum_{m=1}^D \left[\frac{\sum_{m=1}^N P_m}{N} \right] \tag{1}$$

$$= P_1 + \frac{P_1 + P_2}{2} + \frac{P_1 + P_2 + P_3}{3} + \dots + \frac{P_1 + P_2 + P_3 + \dots + P_{365}}{365} \tag{2}$$

$$= P_1 \left(1 + \frac{1}{2} + \frac{1}{3} + \dots + \frac{1}{365} \right) + P_2 \left(\frac{1}{2} + \frac{1}{3} + \dots + \frac{1}{365} \right) + \dots + P_{365} \left(\frac{1}{365} \right) \tag{3}$$

The normalized form of Eqs. (1–3) is used to represent the WRI per day viz:

$$WRI_i = \frac{P_{E_i}}{W} = P_1 + \frac{\{P_2(W-1)\}}{W} + \frac{\left\{ P_3 \left(W-1-\frac{1}{2} \right) \right\}}{W} + \frac{\left\{ P_4 \left(W-1-\frac{1}{2}-\frac{1}{3} \right) \right\}}{W} + \dots + \frac{\left\{ P_{365} \left(W-1-\frac{1}{2}-\dots-\frac{1}{365} \right) \right\}}{W} \tag{4}$$

Note that $(W \equiv 1 + \frac{1}{2} + \frac{1}{3} + \dots + \frac{1}{365})$ is a weighting factor summed over an annual precipitation cycle developed in Byun and Wilhite (1999) and used in other studies (e.g., (Deo et al. 2015; Nosrati et al. 2011). It considers the contribution strength of earlier day P applied in the context of flood risk monitoring (Lu 2009).

¹ The concept of “water resources” in this study is interpreted in the context of accumulated precipitation over time and therefore precludes other forms of water resources (e.g., drinking water, ground water, agricultural, industrial, household, recreational and environmental activities).

Table 1 Hydrological statistics for study locations averaged from 1998 to 2013 (Dobong Observatory, South Korea) and 2008 to 2013 (Brisbane River at Linville, Australia)

ID	Station name	Location	Elevation (m)	Missing data	Precipitation, P (mm year ⁻¹)			
					Mean	Standard deviation	Max	Min
Weather stations								
143007A	Brisbane River at Linville	26.804° S, 152.274° E	124	0.12%	864.5	281.4	1202.0 (January 2011)	568.0
47406	Dobong Observatory	37.666° N, 127.029° E	55.5	Estimated by the government ^a	1642.5	305.6	2273.0 (August 1998)	1206.0
Hydrological stations								
					Hourly river heights, H (m) based on hourly data			
					Mean	Standard deviation	Max	Min
143007A	Brisbane River at Linville	26.804° S, 152.274° E	124	0.69%	0.56	0.51	11.05 [11 Jan 2011 at 5 am]	0.07
1018675	Jungryang River	37.583° N, 127.067° E	55	10.18%	0.58	0.56	6.55 [06 Aug 1998 at 7 am]	-0.05
					Brisbane river discharge rate, Q_{DR} (ml h ⁻¹)			
					27.65	0.49	1.55 × 10 ⁴ [11 Jan 2011 at 5 am]	0

Only the discharge rate data for the Brisbane River were available

^a Information on the actual method of data recovery not readily available

Equation (4) illustrates mathematically how the raw P_m is objectively converted to P_E for any i th day, where the antecedent P is represented in a rational manner with reduced weighting to accommodate for the loss of water resources over the passage of time. A similar notion is utilized in earlier studies on flood and drought analysis (Byun and Wilhite 1999; Deo et al. 2015; Lu 2009, 2012; Lu et al. 2013; Lu et al. 2015; Nosrati et al. 2011).

According to Eq. (4), P_E is likely to represent all rainfall received on the i th day, $\approx 85\%$ on the day ($i - 1$), $\approx 77\%$ on the day ($i - 2$), and so on, up to $\approx 0.0423\%$ on the day ($i - 365$). Note that here, we are considering a summation period up to an annual cycle.² However, the 365 days used in Eq. (4) can be extended to more days when the wet season continues for more than 1 year, as shown in Byun and Wilhite (1999).

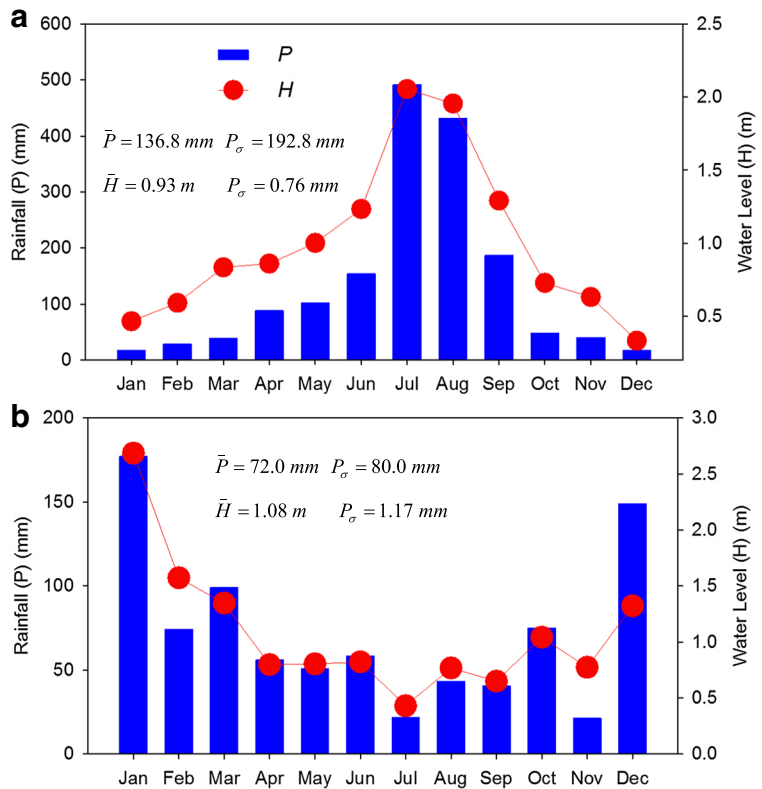
A statistical representation of weighted-rainfall accumulation is employed in an objective manner to account for the diminishing contribution of P_m into a volume of water by hydrological factors (e.g., runoff, evapotranspiration, percolation, discharge) that can moderate the

flood extent (Byun and Lee 2002; Kim et al. 2009). This notion concurs with the physical principle for depletion in water resources incorporated in rainfall–runoff models (Jakeman and Hornberger 1993; Lee and Huang 2013), daily assessment of flood risk (Deo et al. 2015; Lu 2009, 2012; Lu et al. 2013; Lu et al. 2015), and the subsequent changes in soil moisture (Yamaguchi and Shinoda 2002). In general, if WRI is sufficiently large, the volume of rainfall accumulation is considered to be relatively high, indicating a larger possibility of a flood (Deo et al. 2015; Han and Byun 2006; Nosrati et al. 2011).

Many studies utilized a daily version of WRI and its subsequent variant for drought and flood assessment (Byun and Wilhite 1999; Deo et al. 2015; Dogan et al. 2012; Kim et al. 2014; Kim et al. 2009; Kim et al. 2011; Lee and Huang 2013; Lee 1998; Lu 2009, 2012; Lu et al. 2013; Oh et al. 2015; Park et al. 2015a; Park et al. 2015b) and the index in its current form is restricted to an assessment of water accumulation for daily time steps. From a practical point of view, a flood event can be better monitored with a mathematical model where hourly rainfall is converted to effective precipitation that is likely to elevate the risk of the event (Arnaud et al.

² For any given leap year, the daily P value for 29 February was added to the P value for 01 March.

Fig. 2 Monthly hydrological cycle with mean and standard deviation of rainfall (\bar{P}, P_σ) and river water level (\bar{H}, H_σ). **a** Dobong Observatory (South Korea; 1998–2013) and **b** Brisbane River at Linville (Queensland; 2008–2013)



2007; Badrzadeh et al. 2015; Econopouly et al. 1990; Toth et al. 2000; Woolhiser and Osborn 1985).

To formulate an hourly metric, a statistical evolution of water volume due to hourly rainfall is proposed. Figure 3 plots the *WRI* for day *i*, *i* – 1 and *i* – 2 (i.e., current day and two antecedent days). In accordance with Eq. (4), maximum water volume accumulated due to P_E is 1 (denoted AD), 0.85 (denoted IJ), and 0.77 (denoted HK) for the current and antecedent 2 days, respectively. Hence, the reflected ratio of hourly rainfall on *WRI* per day, where the likelihood of a flood risk is based on the redistributed rainfall per day, is proposed.

In Fig. 3, let us consider rectangle ABCD where the quantity of accumulated water volume in terms of the area covered for this day (1) is 3.60 (i.e., $24 \times (1 - 0.85)$). Since line segment CD and AE have equal sizes (≈ 0.15), the coordinate (*t*, *WRI*) at point C and point E are positioned at (25, 0.85) and (1, 1.15). By this analogy, the area of triangle BCE is equal to the area of rectangular ABCD (in other words, the quantity of water (≈ 3.60), for day 1, is identical to the redistributed value stipulated in triangle BCE).

In accordance with earlier research (Deo et al. 2015; Kim et al. 2009; Nosrati et al. 2011), the remaining quantity of water at point C positioned at the end of 24 h for day 1, is estimated to be $\approx 85\%$ of the quantity at point A (100% at the start of the day) to satisfy Eqs. (1–3). Following the principles stipulated in Deo et al. (2015) and Lu (2009), a time-dependent function is applied to estimate the hourly water in terms of the redistributed rainfall per hour. Consequently, the remaining water redistributed over a 24 hourly period is proposed as:

$$P_{E-hr} = \sum_{t=1}^{24} [P_{hr_t} \times (-0.0125t + 1.1625)] \tag{5}$$

where P_{hr_t} = hourly rainfall at the respective time-scale, *t* (hours), and P_{E-hr} = hourly effective precipitation over a duration of 1 to 24 h that represents the redistributed water resources for this period.

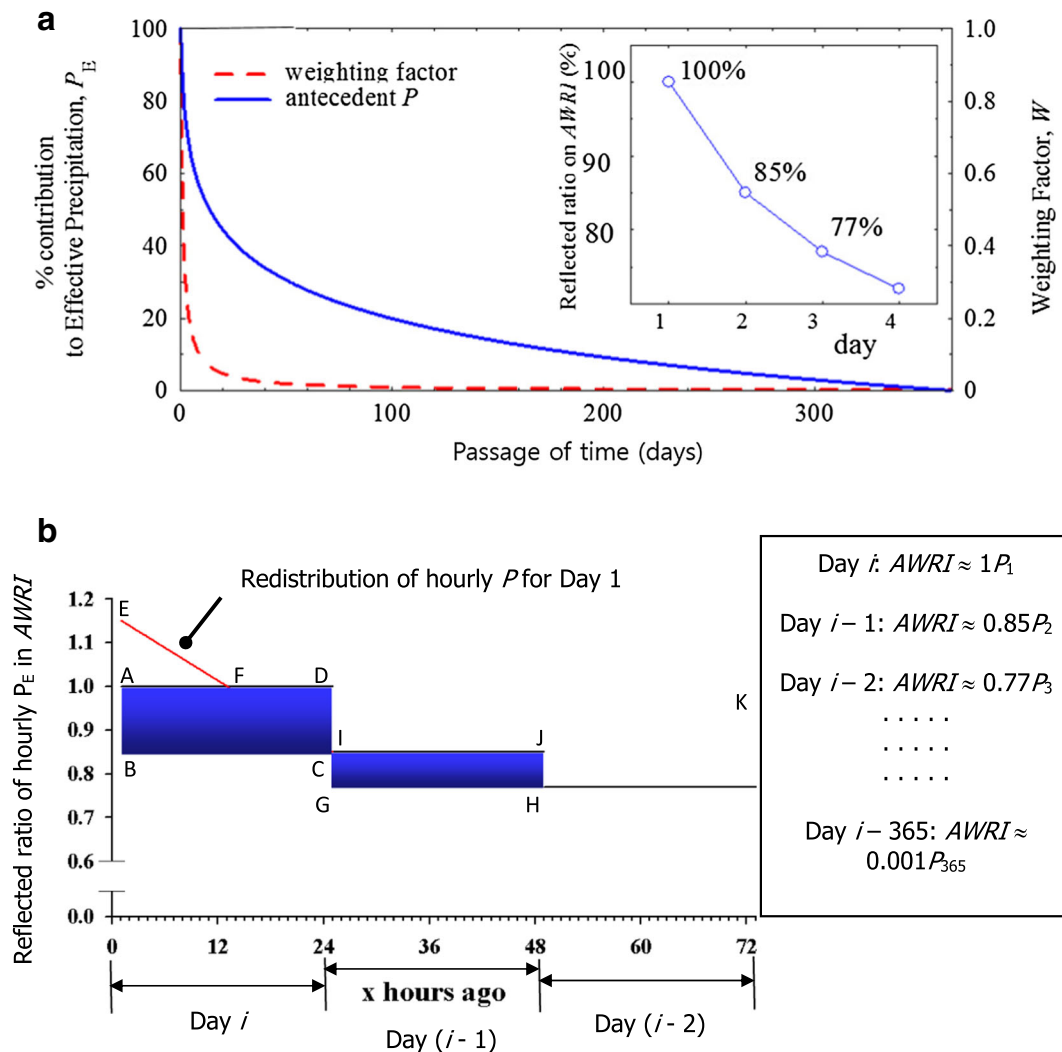


Fig. 3 a Representation of the weighted contribution of daily precipitation (P) converted to effective precipitation (P_E) for annual cycle ($N=365$ days). b Reflected ratio of P_i on Available Water Resources Index ($AWRI$) per day, with the redistributed hourly precipitation for each i th day where reflected ratio of P_E

into $AWRI$ is ≈ 1.00 for $AWRI$ at the start of day i ($t=1$ h) but 1.15 represented by long-term water resources index (WRI_{hr-L}). Ratio of P_E is 1.00 (day i), ≈ 0.85 (day $i-1$), ≈ 0.77 (day $i-2$), ..., 0.001 (day $i-365$) in accordance with daily flood monitoring (Byun and Lee 2002; Deo et al. 2015; Kim et al. 2009)

The hourly long-term water resources index (WRI_{hr-L}) is written as:

$$WRI_{hr-L} = \frac{P_{E-hr}}{W} = P_{E-hr} + 0.85P_{E-hr} + 0.77P_{E-hr} + \dots + 0.0423P_{E-hr} \quad (6)$$

It is important that WRI_{hr-L} incorporates the role of antecedent and current rainfall and, therefore, can assess the surplus/deficit of water with a combination of duration and accumulated amounts.

While the metric stipulated in Eq. (6) can be useful for detecting the flood risk caused by rainfall accumulations over the long-term (i.e., weighted summations over an annual cycle), a robust index for the short-term risk assessment is more suitable for studying the possibility of flash floods. Often, the onset of a flash flood is noted with short lead time warning (i.e., less than a few hours) (Lumbroso and Gaume 2012; Ruiz-Villanueva et al. 2012). In order to develop a short-term metric, a modified version of Eq.

(6), termed the hourly short-term water resources index ($WRI_{24\text{-hr-s}}$), is proposed:

$$WRI_{24\text{-hr-s}} = \frac{P_{E-24hr}}{W_{24hr}} = P_1 + \frac{\{P_2(W_{24hr}-1)\}}{W_{24hr}} + \frac{\left\{P_3\left(W_{24hr}-1-\frac{1}{2}\right)\right\}}{W_{24hr}} + \frac{\left\{P_4\left(W_{24hr}-1-\frac{1}{2}-\frac{1}{3}\right)\right\}}{W_{24hr}} + \dots (7)$$

$$\dots + \frac{\left\{P_{24}\left(W_{24hr}-1-\frac{1}{2}-\dots-\frac{1}{24}\right)\right\}}{W_{24hr}}$$

Here, the rainfall input is now m “hours” before instead of m “days” in a 24-h period, and the weighting factor ($W \equiv 3.816$) incorporates the contribution of accumulated rainfall in the latest 24 h. Alternative forms of the short-term water resources index ($WRI_{D\text{-hr-s}}$) are proposed with different summation (or rainfall accumulation) D time steps. For example, a 48 hourly period, $WRI_{48\text{-hr-s}}$ ($W \equiv 3.479$ with $D = 48$ h), 72 hourly period, $WRI_{72\text{-hr-s}}$ ($W \equiv 4.875$ with $D = 72$ h), 96 hourly period, $WRI_{96\text{-hr-s}}$ ($W \equiv 5.517$ with $D = 96$ h) and a 168 hourly period, $WRI_{168\text{-hr-s}}$ ($W \equiv 5.710$ with $D = 168$ h), are utilized to further assess the flood risk based on different summation (D) time steps. These alternative formulations are able to yield crucial information on the risk of the flood event based on different durations and respective rainfall accumulations.

The respective time step used to represent different W is designed to ensure that the decay of a flood effect due to runoff, evapotranspiration, drainage, percolation, etc., is considered, in accordance with the “weighted average precipitation” (Lu 2009). It is imperative to note that the proposed conversion of hourly rainfall into a water resources index aims to standardize the hourly rainfall into non-zero rainfall values in the respective flood (or non-flood) period. Consequently, the proposed metric WRI_{hr} presents a distinct advantage over raw hourly rainfall data used for flood risk assessments (which are likely to contain zero values when measured over an hourly time step).

Results and discussion

Results

The results of the hourly water resources index for flood risk monitoring are presented for flood-prone sites (Dobong Observatory, South Korea; Brisbane River at

Linville, Australia) (Fig. 1). Although both sites were subjected to a number of floods recorded in the hydrological data series, the analysis period was from 1998 to 2002 and 2009 to 2013, respectively, as these coincided with major flooding events in both nations. To validate the water resources index, the time series, power spectrums, and wavelet transformations representing the evolution of flood events are assessed.

In order to identify periods of major flooding in the hydrological data series, we identified flood risk periods using the maximum monthly long-term hourly water resources index (WRI_{hr-L}) and its evolution relative to peak water level and precipitation for the two study sites. Figure 4 plots a time series of the monthly maximum precipitation (P_{max}) with the maximum value of WRI_{hr-L} and H . In order to verify the correspondence of WRI_{hr-L} with the flood extent, the hydrological state of the sites, in terms of the mean river water level (H), were included. Note WRI_{hr-L} was computed using hourly rainfall totals by applying a long-term summation period ($D = 365$ days) and appropriate weightings to the antecedent hourly rainfall following Eq. (6). Therefore, this parameter can be interpreted as a quantitative measure of the long-term remaining water resources in relation to the risk of a flood event for a given month. While comparisons of WRI_{hr-L} with H were possible at the same site for the Brisbane River, the H data compared with flood conditions for Dobong Observatory were recorded at a small distance (≈ 9.82 km) away, known as the Jungryang Bridge.

The hydrographs for the study sites (Fig. 4a, b) showed that the precipitation per month was very much in-phase with the hourly $WRI_{24\text{-hr}}$ per month and river water levels (H) over the respective period of study, confirmed by a two-tailed Kolmogorov-Simonov test at a significance level of $\alpha = 0.05$. Consequently, the precipitation and H data also exhibited a harmonic variation with the magnitude of WRI_{hr-L} . Any changes in monthly rainfall were mirrored by the respective changes in the magnitude of the WRI_{hr-L} , as well as the recorded heights of the mean water level in the river system. For the flood events analyzed at the Dobong Observatory site (Fig. 4a), there was evidence of strong seasonality in the monthly flood patterns, where the month of August showed the largest recorded rainfall ($P_{max} \approx 344.40$ mm) and correspondingly, the largest magnitude of the long-term water resources index ($WRI_{hr-L} \approx 22,595.22$ mm). Interestingly, the river water levels at the Jungryang Bridge in August 1998 were also

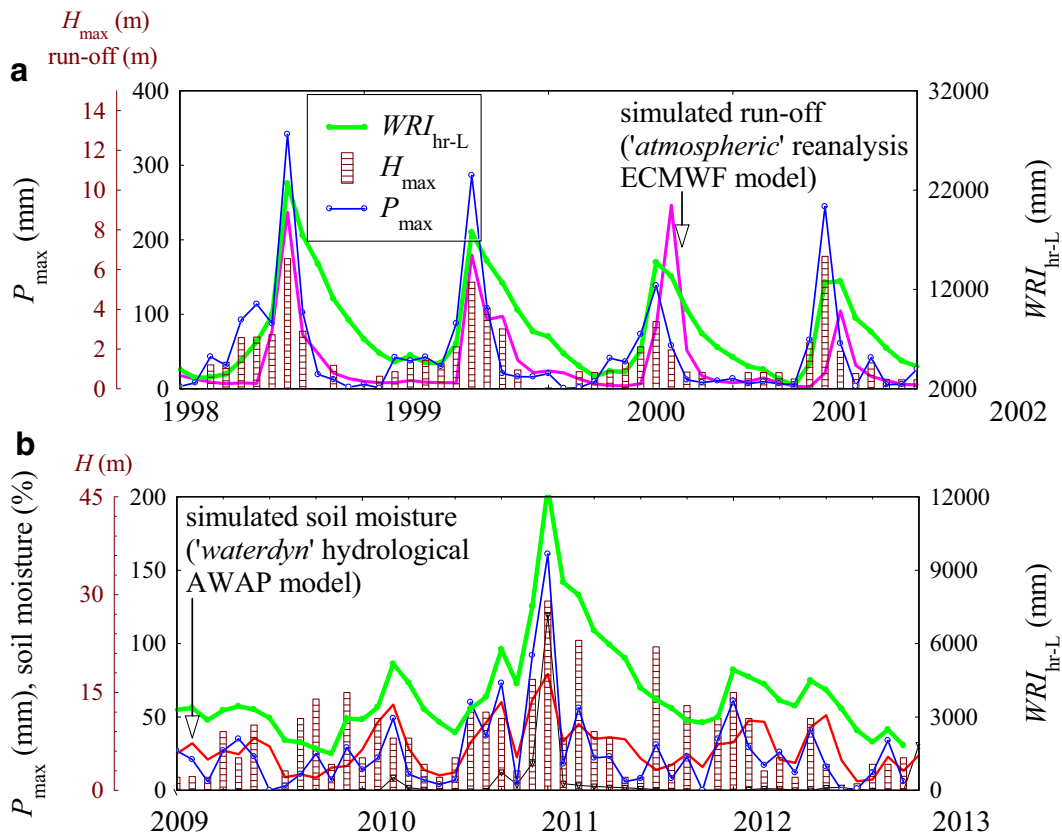


Fig. 4 Identifying flood risk periods using the maximum monthly long-term hourly water resources index (WRI_{hr-L}), peak monthly water level (H_{max}), and monthly maximum precipitation (P_{max}). **a** Dobong Observatory, South Korea. **b** Brisbane River (Linville,

Australia). Simulated surface runoff data (from the atmospheric reanalysis model for Dobong Observatory) and soil moisture data (from the *Waterdyn* AWAP model for Brisbane River) are also shown (Dee et al. 2011; Raupach et al. 2009)

relatively high ($H \approx 6.55$ m) when compared to the other months for the same site.

In contrast, the temporal patterns of monthly floods identified for the Brisbane River site was rather different and not as distinct in terms of its seasonality compared to the patterns for the Dobong Observatory site. Closer examination also showed that the most severe flood events, in terms of their highest recorded maximum rainfall, occurred in December 2010; this period also had the highest (peak) value of the accumulated monthly water resources quantified by Eq. (6) as well as an elevated height of the Brisbane River water level. When compared with the other flood events within the Brisbane River site during the period 2009–2013, this event clearly outweighed the severity encountered in past events. Therefore, it can be ascertained that the wet periods in August 1998 and December 2010 were the most vulnerable months for Dobong Observatory

and Brisbane River sites, respectively. Notwithstanding this, it is important to mention that the prevalence of severe flooding events within this period of study was effectively captured by the monthly long-term water resources index. A similar deduction can be made by comparing the long-term water resources index with water levels in the river systems.

Figure 5a, b displays a scatterplot of daily totals of the hourly short-term water resources index (WRI_{D-hr-S}) versus rainfall (P_{hr}) accumulated for $D = 24, 48,$ and 72 hourly summation periods. Also included in each panel is the square of the regression coefficient (r^2) at various time steps considered for daily flood analysis. The highest correlations ($r^2 \approx 0.906$ and 0.839) were obtained for the case when the short-term water resources were quantified over a 24-h period at both hydrological sites. However, the level of correlation between $WRI_{24-hr-S}$ and P_{hr} was approximately 10% higher for the Dobong

Observatory site when compared with the Brisbane River site. Although the difference was small, this indicated that the flood metric was able to represent the flood events more precisely for Dobong Observatory compared to the Brisbane River site. For both sites, the magnitude of the r^2 appeared to decrease when the summation period for hourly rainfall increased; the magnitude of the r^2 decreased from 0.906 to 0.662 (for the Dobong Observatory) and 0.839 to 0.546 (for the Brisbane River) when the summation period was changed from a 24 hourly to a 72 hourly time step. This confirms that the most recent rainfall was accumulated into much of the water resources; however, with the passage of time, this water volume dissipated gradually and, therefore, was poorly correlated with hourly rainfall data for longer time steps represented in the depletion function (Eq. 7).

Hydrological data series (e.g., water resources index) exhibit large- and small-scale periodic, random, and stochastic variations in time and frequency domains (Khaliq et al. 2006). Hence, a versatile flood risk metric must detect the repetitive phenomenon in a flood metric relative to those present in rainfall data. Hence, we employed the discrete wavelet transform (DWT) algorithm (Mallat 1989, 1998) to verify the frequency components present in $WRI_{24\text{-hr-S}}$ in relation to the P_{hr} and H data. Note that P_{hr} and H are the raw hourly rainfall and river heights whereas $WRI_{24\text{-hr-S}}$ is the water resources index based on rainfall accumulations with a summation period of $D = 24$ h. The DWT process allowed for an examination of the localized modulations in scale (inverse of frequency, analogous to period) and amplitudes of $WRI_{24\text{-hr-S}}$ that was not possible with traditional hydrographs. A dyadic grid was developed where discrete wavelet coefficients (DWC) corresponding to powers of two were chosen to decompose the signal (P_{hr} , $WRI_{24\text{-hr-S}}$, and H) viz (Mallat 1998):

$$\Psi_{m,n}\left(\frac{t-s}{r}\right) = r_o^{-\frac{m}{2}} \Psi^*\left(\frac{t-ns_o+r_o^m}{r_o^m}\right) \tag{8}$$

A level of similarity was identified using Daubechies-5 mother wavelet function, $\Psi_{m,n}$ at different scales and translation periods where $m, n =$ integers that denote the magnitude of wavelet compression/expansion and translation, respectively, ($r_o > 1$) = specified dilation step and ($s_o > 0$) = location parameter.

Assuming $r_o = 2$ and $s_o = 1$, the DWT function was given by (Kisi and Cimen 2011):

$$Z_f(m, n) = 2^{-m/2} \sum_{t=0}^{N-1} F(t) \Psi^*(2^{-m}t-n) \tag{9}$$

where $Z_f(m, n) =$ wavelet coefficient, $F(t)$ is a finite (raw) time series that needs to be decomposed ($t = 0, 1, 2, \dots, N - 1$), $n =$ time translation parameter between $0 < n < 2^{M-m} - 1$, and $m =$ magnitude compression/expansion parameter ($1 < m < M$) (Fig. 6).

Figure 5 illustrates DWCs generated from hourly precipitation (P_{hr}) and the short-term water resources index ($WRI_{24\text{-hr-S}}$) at one level of approximation and four levels of detail for Dobong Observatory. It was noteworthy that large-scale frequencies contained in $WRI_{24\text{-hr-S}}$ (denoted by approximation A3) were in good agreement with frequencies in $P_{24\text{hr}}$, and both were in close parity with the original rainfall data. The small-scale (detailed) frequency components (D1, D2, ... D5) were also in-phase. Taken together, this illustration confirms that the progression of flood risk based on both the low and the high frequency information in hourly rainfall data are well represented in the hourly water resources index.

For a statistical evaluation of the $WRI_{24\text{-hr-S}}$ in relation to its skill for flood risk monitoring, we assessed the cross correlation coefficient (r_{cross}) between DWCs of hourly rainfall and hourly river water level with the DWCs of WRI_{hr} for the Brisbane River (Linville) using the data from November 2010 to January 2011. It is important to mention that cross correlations measured the similarity between $WRI_{24\text{hr}}$ and shifted (lagged) copies of P_{hr} and H .

For a real-time series, $x_i = (x_1, x_2 \dots x_{M-1})$ and $y = (y_1, y_2 \dots y_{N-1})$, the covariance is given by (Deo et al. 2017):

$$\phi_{xy,k} = \frac{\sum_{j=\max(0,k)}^{\min(M-1+k,N-1)} x_{j-k} y_j}{\sqrt{\phi_{xx}(0)\phi_{yy}(0)}} \tag{10}$$

where the cross correlation coefficient, r_{cross} is defined as

$$r_{\text{cross}}(t) = \frac{\phi_{xy}(t)}{\sqrt{\phi_{xx}(0)\phi_{yy}(0)}} \tag{11}$$

such that the quantity $r_{\text{cross}}(t)$ is expected to vary between -1 and 1 .

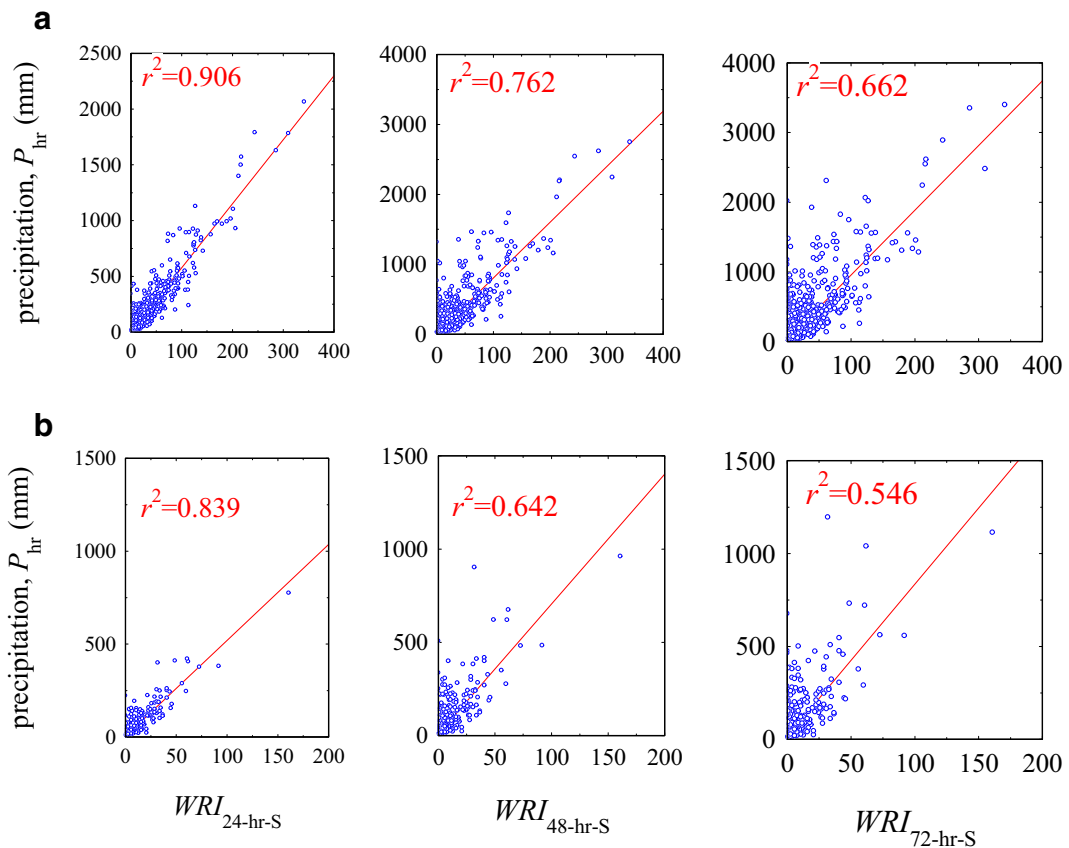


Fig. 5 Scatterplot of daily total of hourly precipitation (P_{hr}) versus the daily water resources index (WRI_{D-hr-S}) for $D = 24, 48,$ and 72 hourly accumulation periods. **a** Dobong Observatory (South Korea). **b** Brisbane River (Linville, Australia)

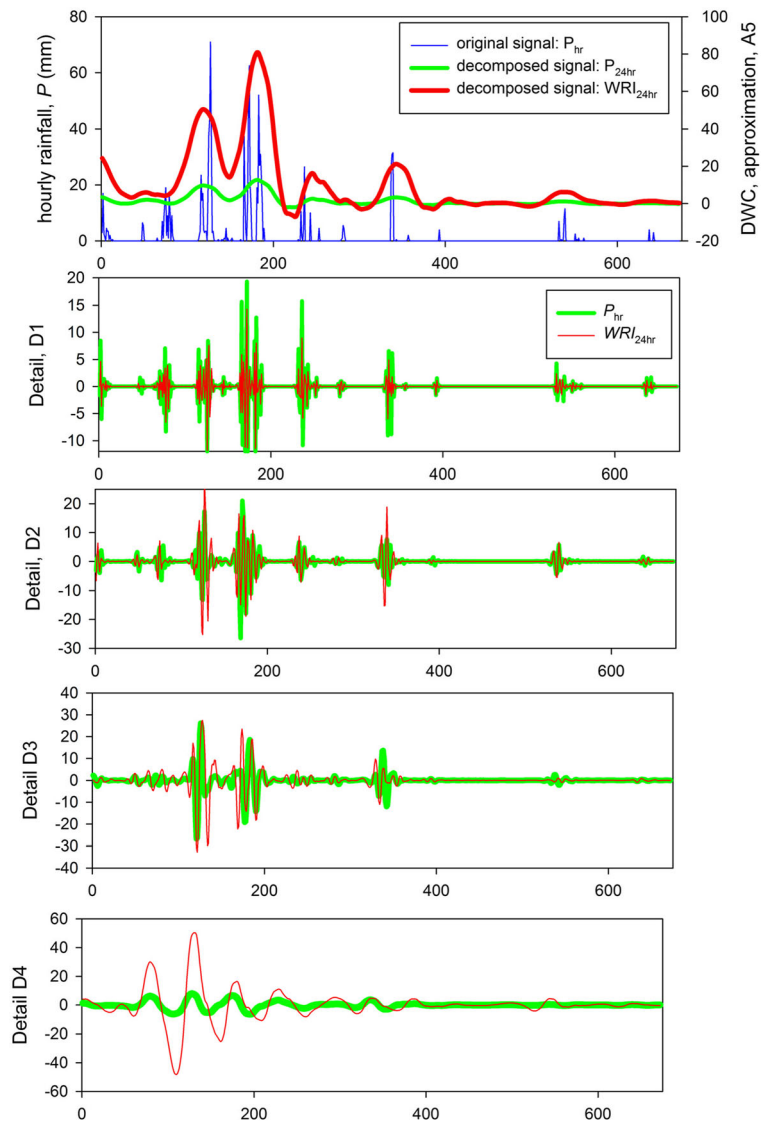
In Table 2, we check the correlation of DWCs acquired from data series of P_{hr} and H with WRI_{D-hr-S} over the short-term ($D = 24, 48, 96, 120,$ and 148 h) and long-term (WRI_{hr-L}) periods for the case of the Brisbane River (Linville) in the November 2010 and January 2011 flood period. As expected, the DWCs yielded the highest degree of correlation between P_{hr} and $WRI_{24-hr-S}$ data series ($r_{cross} \approx 0.703\text{--}0.959$), indicating that the largest amount of water resources emanates from the rainfall accumulated from the recent 24-h period (Table 2). However, based on wavelet-decomposed DWCs, the highest degree of correlation between P_{hr} and $WRI_{24-hr-S}$ was obtained for the largest-scale approximation term ($r_{cross} \approx 0.959$), followed by its respective detailed components D1 (≈ 0.910), D2, and D3 ($\approx 0.608\text{--}0.626$) and D4 and D5 (≈ 0.703).

It was also interesting to note that the level of correlation, as determined by low and high frequency DWCs, decreased gradually as the time step of the water accumulation period was increased. This agreed with the

mathematical formulation of the decay in water resources over the passage of time (Eqs. 1–7). Hence, when correlations of the DWCs of hourly rainfall with long-term water resources were assessed, the magnitude of r_{cross} yielded 0.107–0.856. Also, the correlation between H and P_{hr} rainfall yielded a relatively large magnitude for approximation terms whereas those for detailed components were very low ($-0.026\text{--}0.095$). This shows that the hourly rainfall data alone is perhaps insufficient to explain the dynamical changes in river water levels and the corresponding possibility of large-scale flooding.

In terms of DWCs acquired from river water level and water resources indices (i.e., Table 2), the correlation of approximation terms and fourth and fifth levels of decompositions were notably high (i.e., 0.567–0.924 and 0.582–0.749, respectively), whereas those for D1, D2, and D3 were low. While this was in fact true for all time steps, the correlation of approximation terms were the highest when the original H and $WRI_{148-hr-S}$ data

Fig. 6 Illustration of the discrete wavelet coefficients (DWCs) generated using discrete wavelet transform (DWT) of the hourly precipitation (P_{hr}) and short-term water resources index ($WRI_{24-hr-S}$) data at one level of approximation and four levels of detailed frequency components for Dobong Observatory (South Korea) in the August 1988 flood event



series were decomposed. Additionally, when the decomposed DWCs for H and WRI_L were considered, the degree of correlation was the highest at the fourth and fifth level of details, which exceeded the magnitudes obtained for DWCs of the P_{hr} and WRI_L data. Therefore, it may be construed that an accurate monitoring of large-scale flood possibility (e.g., river floods) should be performed using long-term water resources accumulations defined by WRI_{hr-L} instead of short-term water resource accumulations (i.e., $WRI_{24-hr-S}$). Overall, the discrete wavelet transform of hourly rainfall, water level, and water resources index had good agreement, confirming the suitability of WRI for monitoring the flood risk.

To explore the measured hydrological parameters and the water resources index, the power spectrum density $\phi(f)$ of hourly precipitation, river water level, and short- and long-term water resources index were computed. A comparison of $\phi(f)$ was interesting, as spectrum analyses can help investigate the regularity and/or periodicity of these discrete signals where different time series possess different power spectral characteristics (Zhou et al. 2002).

Figure 7 compares the $\phi(f)$ plot where hourly precipitation with the short-term water resources index for Dobong Observatory and the hourly river water levels with the long-term water resources index for the Brisbane River (Linville, Australia) are shown. It is

Table 2 Cross-correlation (r) between discrete wavelet transform coefficients of (a) hourly rainfall (P_{hr}) versus short and long-term water resources index (WRI_{D-hr}) and (b) river water levels (H)

versus WRI_{D-hr} for the Brisbane River (Linville) at different time steps (D) for data between November 2010 and January 2011

(a)							
Level of decomposition	P vs. WRI_{D-hr}						
	P_{hr} vs. $WRI_{24-hr-S}$	P_{hr} vs. $WRI_{48-hr-S}$	P_{hr} vs. $WRI_{96-hr-S}$	P_{hr} vs. $WRI_{120-hr-S}$	P_{hr} vs. $WRI_{148-hr-S}$	P_{hr} vs. WRI_{hr-L}	P_{hr} vs. H
Approximation	0.959	0.901	0.859	0.824	0.791	0.256	0.736
Detail, D1	0.910	0.904	0.901	0.899	0.897	0.856	-0.145
D2	0.626	0.590	0.572	0.562	0.555	0.371	-0.026
D3	0.608	0.554	0.532	0.517	0.507	0.270	-0.193
D4	0.703	0.540	0.491	0.447	0.422	0.107	0.095
D5	0.703	0.540	0.491	0.447	0.422	0.107	0.095
(b)							
	H vs. WRI_{D-hr}						
	H vs. $WRI_{24-hr-S}$	H vs. $WRI_{48-hr-S}$	H vs. $WRI_{96-hr-S}$	H vs. $WRI_{120-hr-S}$	H vs. $WRI_{148-hr-S}$	H vs. WRI_{24-L}	
Approximation	0.813	0.869	0.907	0.921	0.924	0.567	
D1	-0.202	-0.202	-0.203	-0.203	-0.203	-0.204	
D2	-0.028	-0.025	-0.025	-0.025	-0.026	-0.011	
D3	-0.036	-0.009	0.000	0.005	0.008	0.068	

illustrated that the dominant peaks in $\phi(f)$ in precipitation and river water level data are mimicked by those of short- and long-term water resources indices.

Based on $\phi(f)$, the spectral coherence function, C_h that compares the power spectrum densities of P_{hr} and H with those of the water resources indices at different time steps, were deduced. C_h was a statistic used to examine the relation between two signals that estimated the power transfer between input (rainfall) and output (water resources index) viz (Labat 2005):

$$C_{x,y}(f) = \frac{|G_{x,y}(f)|^2}{G_{xx}(f) G_{yy}(f)} \tag{12}$$

where the signal, $x(t)$ was denoted by P_{24hr} and H and $y(t)$ was the WRI_{hr} at various time steps and $G_{x,y}(f)$ was the cross-spectral density between x and y and $G_{xx}(f)$ and $G_{yy}(f)$ were the auto-spectral densities of x and y , respectively.

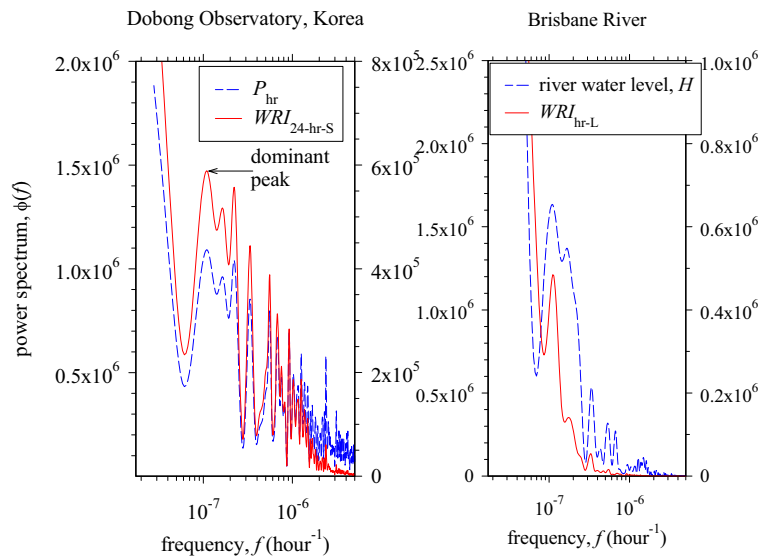
For both sites, the mean spectral coherence function registered a magnitude of $C_h = 0.999$ for the case of P_{24hr} and WRI_{24-hr} , with a standard deviation of zero. As the summation time step was increased from 48 to 72 h, the magnitude of C_h decreased gradually to $C_h \approx 0.705$, with a standard deviation of 0.217 (Dobong) and $C_h \approx 0.996$ with a standard deviation of 0.001 (Brisbane). It is noteworthy that when the spectral coherence

of river water levels were compared with those of the water resources indices, a significantly lower spectral coherence and larger standard deviation was obtained. In terms of the coherence of the long-term water resources index, a magnitude of $C_h \approx 0.785$ was obtained for Dobong, whereas a relatively larger value was obtained for Brisbane ($C_h \approx 0.996$). Although it was not clear, this indicates that the hourly rainfall accumulation correlates better with the long-term water resources index for Brisbane compared to Dobong.

In Fig. 8, an analysis of the temporal evolution of flood based on changes in hourly long-term (WRI_{hr-L}) and hourly short-term (24 hourly) water resources index ($WRI_{24-hr-S}$) for the heavy rainfall period (4th–9th August 1998) at Dobong Observatory site was performed. The bars denote the hourly rainfall, while the red shows the $WRI_{24-hr-S}$, blue shows the WRI_{hr-L} , and the shading part represents the mean water level (H) at the Jungryang Bridge site. It can be seen that the period of analysis included four major heavy rainfall events (indicated by the bar plot), where two occurred on the 4th and 6th of August, and the other two rainfall events were separated by just a few hours on the 8th of August.

When hours of heavy rainfall were compared with the short-term water resources index, changes in P_{hr} appear to be well correlated with changes in $WRI_{24-hr-S}$, but of

Fig. 7 A comparison of the power spectrum, $\phi(f)$ for a hourly precipitation (P_{hr}) with the short-term water resources index ($WRI_{24-hr-S}$) for the case of Dobong Observatory (South Korea) and **b** hourly river water level (H) with the long-term water resources index (WRI_{hr-L}) for Brisbane River (Linville, Australia)



course, the magnitude of $WRI_{24-hr-S}$ does not include zero values as this represents the rainfall accumulated index. When the P_{hr} and $WRI_{24-hr-S}$ were compared via the two-tailed Kolmogorov-Simonov test at a significance level of $\alpha = 0.05$, the results confirmed that both data distributions followed similar patterns. In fact, the pattern of change for the curve representing the short-term WRI was close to the pattern representing the hourly rainfall

changes, as well the pattern of water levels recorded at the Jungryang Bridge site. It was also clear that, although there were several zeros in the raw hourly rainfall, no zero values were present in the computed water resources index, and all hours were represented by their unique values of WRI_{hr} . Clearly, the standardized form of the WRI_{hr} without zeros is a distinct advantage of the flood risk assessment metric.

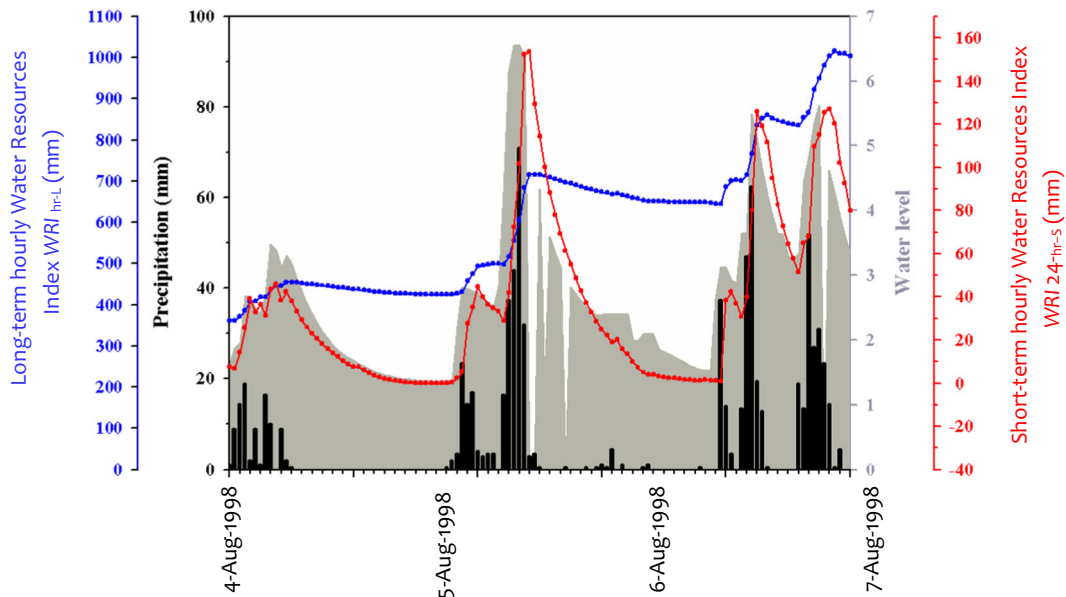


Fig. 8 Hourly monitoring of the flood risk based on the long-term water resources index (WRI_{hr-L}) and the short-term water resources index ($WRI_{24-hr-S}$) for Dobong Observatory (South Korea from 4th to 9th August 1998. Bars denote the hourly precipitation data (P_{hr})

whereas the red line depicts the respective changes in $WRI_{24-hr-S}$, the blue line shows WRI_{hr-L} , and the shaded plot represents the hourly water level (H) for Jungryang Stream. Units: in mm except water level (m)

A closer scrutiny of the hourly rainfall bar graph showed that the period from the 4th of August (at 1300 hours) to the 5th of August (at 1600 hours) was almost rainless. Following this relief in rainfall activity, the magnitude of $WRI_{24\text{-hr-S}}$ dropped from approximately 29.23 to 0 mm. However, the rate of decline in water resources was gradual and was concordant with Eq. (7). In fact, the magnitude of $WRI_{24\text{-hr-S}}$ only reached zero value at about 1200 hours on the 5th of August, although no rain water was received from the 4th of August (1300 hours). It was interesting to note that within this dry period, the water resources calculated over the 48 to 72 hourly summation periods exhibited a much lower decay rate than when the antecedent period of consideration was made longer. Also, the response of changing rainfall over hourly times scales was much weaker for the $WRI_{\text{hr-L}}$, as this index also utilized a lengthier antecedent period.

In agreement with earlier studies (Glade 1998; Ma et al. 2014; Zêzere et al. 2008), a practicality of WRI_{hr} is demonstrated by checking its relationship with the short- and long-term WRI and subsequent heavy rainfall disasters in the vicinity of Dobong Observatory. To provide an explanation on how the heavy rainfall disasters correspond to the WRI , anecdotal records of water-related disasters between the 4th and 8th of August 1998 were gathered from the most reliable sources (HRFCO 2014; Lee and Hur 2000; MOLIT 1999, 2014; Yonhapnews 1998, 2004). While an exhaustive list of all disasters in this period was not available, notable disasters in terms of extended evacuation, inundations, flash floods, and landslides were gathered. Table 2 shows the water-related disaster, as well as the long ($WRI_{\text{hr-L}}$) and short-term water resources index ($WRI_{24\text{-hr-S}}$), including the time of the occurrence of this event.

From the 4th to the 7th of August, there was a gradual increase in the magnitude of the hourly $WRI_{\text{hr-L}}$, which coincided with a number of water-related disasters. Explicitly, a flood event was observed in Jungryang Stream at 0800 hours on the 4th of August, when the magnitude of $WRI_{\text{hr-L}}$ was approximately 436.00 mm. Likewise, the Eastern Trunk Road was inundated at 0428 hours on the 6th of August when the magnitude of the $WRI_{\text{hr-L}}$ increased to approximately 497 mm. After this notable event, major water-related disasters followed on the 6th of August within the 0557–0800 hour period. During this time, $WRI_{\text{hr-L}}$ increased from approximately 556 to 683 mm.

A major inundation event was also recorded at the Dobong Train Station at this time, resulting in a complete halt of the Subway-7 Train Services at about 0557 hours, followed by a major landslide event at U-ie Dong at about 0800 hours on the 6th of August. For these two water-related disasters, the recorded hourly rainfall was approximately 37.5 and 71.0 mm, respectively, and the respective corresponding $WRI_{\text{hr-S}}$ was approximately 72 and 152 mm. It was observed that the short-term accumulation of rainfall was a good indicator of inundation and landslide events, as it considered the cumulative rainfall over the most recent 24 h period that was sufficient to trigger these water-related disasters.

Based on Fig. 8 and Table 3, a number of water-related disasters were persistent between 0330 hours and 1930 hours, which coincided with elevated WRI . For example, at 0330 hours, a flood event was reported in the vicinity of the Banghak Stream, which was followed by a landslide, soil runoff and an inundation event in neighboring areas. This led to the closure of the Eastern Trunk Road when the magnitude of the hourly $WRI_{\text{hr-L}}$ was approximately 714 mm. A landslide was reported in Chang-Dong region, and the Dobong Station lobby (i.e., 2nd full stop of Subway-7) was inundated, with a provisional levee (50 m) of the Dobong Stream being washed away when the magnitude of the hourly $WRI_{\text{hr-L}}$ was approximately 835 mm at 0500 hours. At 0800 hours on the 6th of August and 0500 hours on the 8th, landslide events were reported. The events coincided with the short-term water resources index having values of 126 and 152 mm, respectively, compared to 40 and 44 mm for flood events at the Jungryang and Banghak streams. A cross-check of hourly rainfall for these events showed that 71.00 mm of rainfall (6th August; 0800 hours) and 62.5 mm (8th August; 0500 hours) was recorded when the major landslides occurred. Based on these observations, it was possible to conclude that the risk of a flood event was largely dependent on the long-term accumulation of water, whereas the risk of a landslide was mostly dependent on highly concentrated rainwater within a 24-h period.

According to Table 3, a very active period of water-related disasters was evident between 0500 hours and 1930 hours on 8th August. To analyze this period closely in relation to the flood monitoring metric, a time series of $WRI_{24\text{-hr-S}}$, $WRI_{\text{hr-L}}$, and hourly precipitation (P_{hr}) for Dobong Observatory in a 24-h period was prepared (Fig. 9). It was interesting to note that the

Table 3 The spectral coherence parameters, $C_h \equiv (P_{hr}, WRI)$ and $C_h \equiv (H, WRI)$ comparing the power spectrum density of hourly precipitation (P_{hr}) and hourly river water level (H) with the short and long-term Water Resources Index (WRI_{D-hr}) for different time steps (D)

(a) Dobong Observatory (South Korea)					
Statistical metric for C_h	P versus WRI_{D-hr}				
	P_{hr} vs. $WRI_{24-hr-S}$	P_{hr} vs. $WRI_{48-hr-S}$	P_{hr} vs. $WRI_{72-hr-S}$	P_{hr} vs. H	P_{hr} vs. WRI_{hr-L}
Mean	0.999	0.996	0.995	0.705	0.785
Standard deviation	0.001	0.002	0.000	0.217	0.146
	H versus WRI_{D-hr}				
	H vs. $WRI_{24-hr-S}$	H vs. $WRI_{48-hr-S}$	H vs. $WRI_{72-hr-S}$	H vs. H	H vs. WRI_{hr-L}
Mean	0.705	0.705	0.705	1	0.627
Standard deviation	0.217	0.217	0.217	1	0.206
(b) Brisbane River (Linville, Australia)					
	P versus WRI_{D-hr}				
	P_{hr} vs. $WRI_{24-hr-S}$	P_{hr} vs. $WRI_{48-hr-S}$	P_{hr} vs. $WRI_{72-hr-S}$	P_{hr} vs. H	P_{hr} vs. WRI_{hr-L}
Mean	0.999	0.997	0.997	0.996	0.996
Standard deviation	0.001	0.002	0.001	0.002	0.003
	H versus WRI_{D-hr}				
	H vs. $WRI_{24-hr-S}$	H vs. $WRI_{48-hr-S}$	H vs. $WRI_{72-hr-S}$	H vs. H	H vs. WRI_{hr-L}
Mean	0.487	0.487	0.487	0.487	0.487
Standard deviation	0.204	0.204	0.204	0.204	0.203

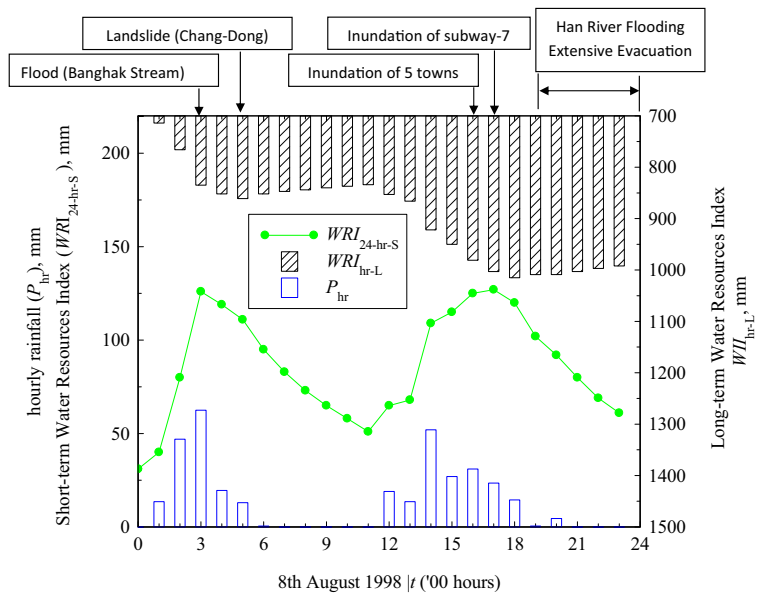
landslide and flood events (which occurred in the early morning of 8th August) appeared to be largely associated with very high values of $WRI_{24-hr-S}$. During this time, the magnitude of the short-term water resources index corresponded well with the torrential rainfall period. However, the magnitude of WRI_{hr-L} for this case was less than 900 mm. It is noteworthy that an inundation of the Subway-7, the evacuation of 1900 residents in five towns, and a major flooding event in the Han River were reported when the magnitude of the WRI_{hr-L} was very high (≈ 852 – 1009 mm) (Fig. 9).

During the large-scale evacuation call by Korean authorities, both the hourly rainfall and short-term water resources index had declined in magnitude, but the long-term water resources index was high (≈ 1000 mm). It can therefore be said that the magnitude of WRI_{hr-L} is an important indicator of the accumulation of water in heavy rainfall events and is therefore a useful tool for flood warning and evacuations. This finding also demonstrates that neither the hourly rainfall amounts nor short-term accumulation of water resources were able to provide sufficient warning of serious water-related disasters such as large-scale flooding. However, the short-term water resources index was useful in the warning of spontaneous, short-term impacts of heavy rainfall (e.g., flood in a stream, landslides and closures of transports or local-scale inundation).

In addition to the above, the suitability of the water resources index for flood monitoring in Brisbane was verified. Figure 9 shows a time series of total precipitation (P_{24hr}), short-term water resources index ($WRI_{24-hr-S}$), and long-term water resources index (WRI_{hr-L}) at a daily time step for severe flood events recorded from 1st December 2010 to 31st January 2011. Note that although $WRI_{24-hr-S}$ and WRI_{hr-L} were originally based on hourly rainfall, their respective equivalents were calculated for the short-term (24 h) and long-term (365 days) periods to verify their suitability for identifying the most severe flood days.

From the 1st to the 18th of December 2010, the recorded daily rainfall was very low (0 – 27 mm day $^{-1}$); however, on the 19th, a heavy rain event resulted in approximately 92 mm of rainfall in just 1 day. In response to this, the magnitude of the short-term water resources index increased to 380.27 mm and the long-term water resources index increased to 5552.66 mm; the $WRI_{24-hr-S}$ was between 0 and 124 mm and the WRI_{hr-L} was between 3586 and 4290 mm prior to this heavy rainfall period. From the 19th of December 2010 to the 9th of January 2011, the rainfall intensity was low, as seen by the relatively low P_{24hr} . As such, the magnitude of $WRI_{24-hr-S}$ continued to fluctuate in response to the subtle changes in rainfall, and a similar pattern was noted for the daily change in the value of WRI_{hr-L} .

Fig. 9 An assessment of the hourly flood risk progression relative to the occurrence of different disaster events recorded on 8th August 1998 for Dobong Observatory (South Korea) using the short-term ($WRI_{24\text{-hr-S}}$) and long-term water resources index ($WRI_{\text{hr-L}}$)



Within the December 2010–January 2011 period, the heaviest rainfall was recorded in the first half of January, with significant floods in Brisbane and Lockyer Valley (Babister and Retallick 2011; Deo et al. 2015; Inquiry 2011). In this study, flooding was clearly evident (Fig. 10), where a sharp increase in the magnitude of the short-term water resources index followed the heavy rainfall period from the 5th to the 11th of January 2011. During this period, the highest daily rainfall total was 161.00 mm (on the 9th of January), which coincided with a rapid increase in the value of $WRI_{24\text{-hr-S}}$ from 97.38 mm (5th January) to 774.39 mm (9th January). The 48 and 72 hourly $WRIs$ were also high on the 9th of January ($WRI_{48\text{-hr-S}} \approx 960.0$ mm and $WRI_{72\text{-hr-S}} \approx 1112.09$ mm, respectively), and the long-term water resources index was approximately 9825.89 mm.

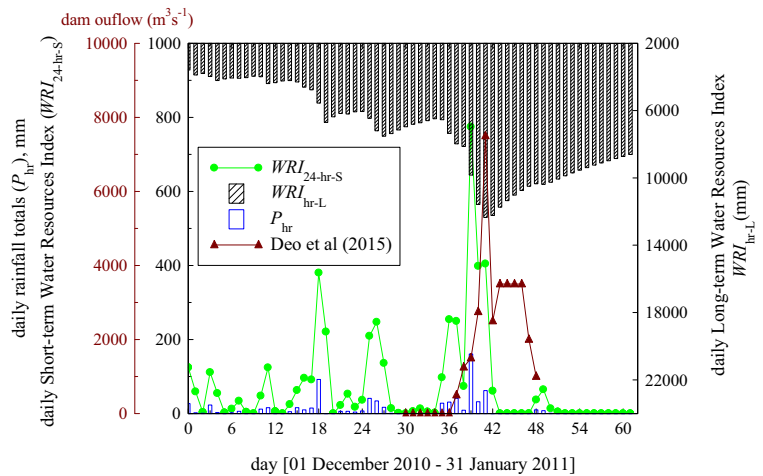
For comparison, the volumetric outflow from the Wivenhoe Dam was included, as it reflected the release of excess water that caused the Brisbane and Lockyer Valley flooding (Deo et al. 2015; van den Honert and McAneney 2011). It was evident that changes of volumetric flow rate closely followed $WRI_{24\text{-hr-S}}$, with a peak on the 11th of January ($Q \approx 7500 \text{ m}^3 \text{ s}^{-1}$) that corresponded to the elevated value of $WRI_{24\text{-hr-L}}$ ($\approx 12,347$ mm). However, the peak Q did not coincide with the occurrence of the maximum value of the short-term WRI , which followed the changes in the hourly P_{hr} more closely. Thus, as in the case of Dobong Observatory, the data indicated that the long-term water resources index may be treated as a robust indicator of large-scale water-

related disasters (e.g., large-scale floods) that could occur due to the very significant accumulation of water resources, whereas the short-term water resources index is a better indicator of short-term water-related disasters (e.g., flash floods). A similar deduction was made for Dobong Observatory (Table 3 and Fig. 9).

For the days identified with a peak risk (9th–10th of January), hourly changes in rainfall, water resources indices, and river water levels were analyzed in order to observe how the flood risk fluctuated during this time. Figure 11 shows the hourly rainfall (P_{hr}) and the $WRIs$ with the corresponding changes in hourly water levels (H). The hourly fluctuations in P_{hr} were very much in phase with the hourly changes in $WRI_{24\text{hr-S}}$. That is, the peak rainfall periods at $t = 0700$ hour ($P_{\text{hr}} \approx 16.00$ mm), 1300–1400 hours ($P_{\text{hr}} \approx 22\text{--}29$ mm) and 1700–1900 hours ($P_{\text{hr}} \approx 11\text{--}13$ mm) were mimicked by corresponding spikes in the magnitudes of the short-term water resources index ($WRI_{24\text{-hr-S}} \approx 25.39, 48.32\text{--}59.52,$ and $51.33\text{--}58.39$ mm, respectively). While the magnitude of $WRI_{\text{hr-L}}$ increased in response to changes in P_{hr} and $WRI_{24\text{-hr-S}}$, it did not attain its maximum value until about midnight ($t = 2400$ hours) on the 9th of January 2011. Interestingly, the height of the river water levels also followed the changes in $WRI_{\text{hr-L}}$, although its peak ($H = 10.11$ m) was detected slightly earlier at approximately 2100 hours.

Another noteworthy point was that the water level, associated with large-scale flooding, was in agreement with hourly changes in the long-term water resources

Fig. 10 Application of the short-term ($WRI_{24\text{-hr-S}}$) and long-term water resources index ($WRI_{\text{hr-L}}$) for daily flood risk analysis in the Brisbane River (Linville, Australia) during the severe flood event in the December 2010–January 2011 period. Also shown is the hourly rainfall (P_{hr}) and literature data for the volumetric outflow (Q) emanating from the Wivenhoe Dam ($\text{m}^3 \text{s}^{-1}$) that was generated by the release of excess stored water in January, 2011 (Deo et al. 2015)



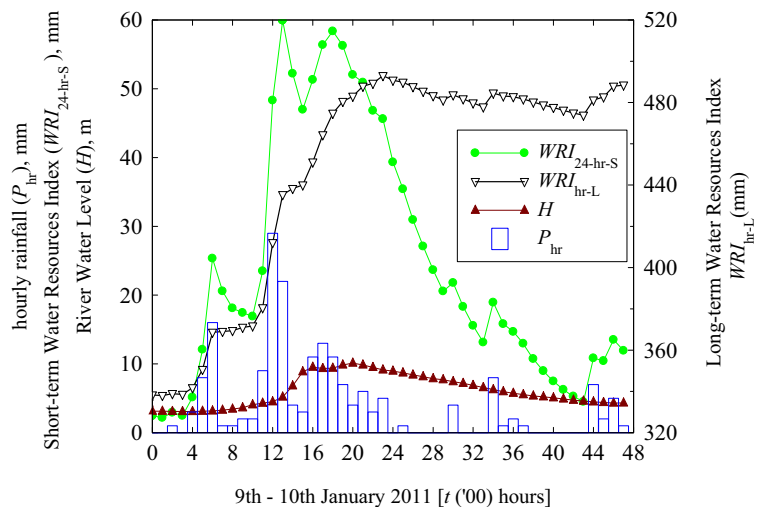
index, and this data distribution was statistically significant through a two-tailed Kolmogorov-Simonov test at a significance level of $\alpha = 0.05$. While a direct comparison of the flood events and its consequences for Brisbane and Dobong Observatory should not be made due to different physiographic factors, the results agree with earlier observations for Dobong Observatory that water-related disasters are well correlated with the magnitude of $WRI_{\text{hr-L}}$ (Table 3; Fig. 9). Consequently, it can be said that the risk of large-scale flooding was deducible from the hourly long-term water resources index, whereas that of short-term flooding (e.g., flash floods) was related to the short-term water resources index.

Figure 11 illustrates a time series of how flood risk evolved in earlier parts of the December 2010–January 2011 event. Also shown are the changes in hourly river water levels, short-term $WRI_{D\text{-hr-S}}$ at various short-term

summation periods (between $D = 24\text{--}148$ h), and long-term WRI , with a 365-day hydrological cycle as the summation period. According to this plot, the danger of a flood could easily be “predicted” by observing the evolution of the water resources indices, which could not be done through observations of rainfall changes in this period. That is, an increasing risk of large-scale flooding was evident from the 1st of December 2010, as the amount of accumulated water resources continued to increase in response to the changes in rainfall.

If one considers only the changes in rainfall, the overall timing of rainfall activity was irregular. In fact, the change in the long-term water resources index (which was non-zero during the entire period) was associated with large-scale flooding and could be monitored to determine the imminent danger of flooding. While river water levels might have also been employed

Fig. 11 Analysis of the hourly changes in long-term water resources index ($WRI_{\text{hr-L}}$), short-term water resources index ($WRI_{24\text{-hr-S}}$), hourly river water level (H), and hourly precipitation (P_{hr}) for the peak flood period (9th–10th January 2011) in Brisbane River (Linville, Australia)



since broad scale patterns are reflected by this hydrological parameter, subtle changes in the magnitude of water level are not easily observable. Furthermore, the WRI s can be computed at any given time step and applied to analyze the dynamical nature of the flood event. Thus, WRI has a distinct advantage over raw rainfall data applied for the monitoring of the progression of an imminent flood event.

The suitability of the proposed WRI was checked in the annual analysis of flood events at the Dobong Observatory. Annual maximum long-term water resources index (WRI_{hr-L}), short-term water resources index ($WRI_{24-hr-S}$), mean rainfall (P_{hr}), and mean hourly water level at Jungryang Bridge for the period 1998–2013 were inspected (Fig. 13). There was very good agreement of WRI s with both the changes in rainfall and river water levels. The years that experienced the most severe flooding were 1998, 2001, 2006, 2009, and 2011. Another observation was that although the mean annual rainfall was very similar during the 1998 and 2003 flood years, the flood severity for these years was different as evidenced by the changes in river water levels and the WRI . In fact, the potential risk of flooding in 1998 significantly outweighed the risk in 2003. Importantly, the river water level was also very high in 1998, which was reflected by the elevated magnitude of WRI_{hr-L} and $WRI_{24-hr-S}$. Another observation was that the year 2006 was highly prone to severe short-term flooding (with large values of the $WRI_{24-hr-S}$) because although the mean rainfall and river water levels were not high, 2006 experienced short-term, torrential rainfall that resulted in a high risk of flash flooding. However, large-scale flooding was unlikely for this year, as the river water levels and long-term water resources index were relatively low.

In order to validate the usefulness of WRI for ranking flood events per month, Tables 4 and 5 show the monthly total rainfall (P_{tot}), long-term WRI , and the short-term WRI at various time steps (24, 48, and 72 hourly) over the period 1998–2013 for Dobong Observatory. The most severe month of flooding was August, with a $P_{tot} \approx 1062$ mm. This resulted in the highest values for WRI_{hr-L} , $WRI_{24-hr-S}$, $WRI_{48-hr-S}$, and the $WRI_{72-hr-S}$. Interestingly, the rank of flood severity based on water resources parameters was consistent with the rank assigned by the total rainfall in the particular month. Also, the rank of flood events by month (Table 3) did not follow the annual ranking of flood severity (Fig. 12), as a given month can possibly have a very severe event,

but overall does not count as a severe flood based on annual-average statistics. This was the case for the July 2006, July 2011, and July 2012 events, which were very severe months of flooding, but were not registered as severe years of flooding. In fact, monthly analysis also showed that the year 2006 experienced a severe flood that was picked up in the annual maximum value of $WRI_{24-hr-S}$ (Fig. 12). It can be seen that the WRI is a versatile statistical measure of flood extent, as it can not only be used for hourly monitoring of flood risk but also for the detection of short- and long-term flood events over monthly and annual timescales.

Discussion

An hourly water resources index (WRI_{hr}) that was derived mathematically was utilized to represent the time-evolution of flood progression based on limited input (rainfall) data as an effective tool for flood risk monitoring. In comparison with other popular methods (e.g., depth-duration-frequency model (Fitzgerald 2007; Gaál et al. 2014), rainfall runoff equations (Jonsdottir et al. 2006), weighted average precipitation (Lu 2009), extreme intensity-duration (Lu et al. 2015), hourly rainfall heterogeneity defined by similarity between hourly and daily rainfall frequency distribution (Martin-Vide 2004)), the WRI_{hr} is easy to calculate, interpret, and apply to hydrological sites where hourly data are readily available. As the WRI_{hr} was also able to convert hourly rainfall of water resources using an objective mathematical measure (Eqs. 1–7) before, during, and after a series of heavy rain events, a continuous time-varying metric was generated. Importantly, the progression of flood danger by this metric was mimicked closely by changes in river water heights, thus validating its utility for flood assessment. The weighting factor applied to account for changes in water resources considered the general effect of the demands of water balance (evaporation, runoff, percolations, etc.), which is in accordance with earlier research (Deo et al. 2015; Lu 2009).

In the context of temporal studies of flood risk, WRI_{hr} offers distinct advantages over other methods (e.g., rainfall–runoff models), as this approach is tailored to operate over hourly rather than daily or monthly time steps, yet it utilizes physical principles similar to “weighted precipitation” in relation to flood risk assessment (Deo et al. 2015; Lu 2009). Moreover, its utility for real-time monitoring of risk is significantly better than earlier studies (Deo et al. 2015; Liu et al. 2015; Lu 2009;

Table 4 Summary of heavy rain and water-related disasters with-in the vicinity of Dobong Observatory (South Korea) from 4th to 8th August 1998 (HRFCO 2014; Lee and Hur 2000; MOLIT 1999, 2014; Yonhapnews 1998, 2004)

Disaster event	WRI_{hr-L}	$WRI_{24-hr-S}$	Local time (August 1998)
Flood in Jungryang Stream	436	44	4th 0800
Eastern Trunk Road inundated	497	29	6th 0428
Inundated Dobong Station (stop of subway-7; recov- ered partly after some time)	556	72	6th 0557
Sand slide in U-ie Dong	683	152	6th 0800
Subway of Euijungbu City Hall inundated again	651	4	7th 0900
(Eastern Trunk Road recovered)	644	1	7th 2230
Flood in Banghak Stream (Land slide, soil runoff and inundation in neighboring area; Eastern Trunk Road closed again at 0240l)	714	40	8th 0330
Landslide in Chang-Dong (Inundation of Dobong Sta- tion lobby-2nd full stop of Subway-7; Recovered after some time; Provisional le- vee (50 m) of Dobong Stream washed away)	835	126	8th 0500
Road of Seoul-Euijungbu closed	852	95	8th 1500
Partial inundation of 5 towns. (Evacuation of 1900 residents)	920	133	8th 1640
Washing away of Jungryang Stream levee, (water level 18.3 m: the danger limit is 17.7 m)	950	115	8th 1710
Increased inundation of Subway-7, 3rd full stop	981	125	8th 1750
(Precautionary flood warning on Han River)	1004	127	8th 1900
(Extended evacuation)	1009	124	8th 1930

The short-term ($WRI_{24-hr-S}$) and long-term water resources index (WRI_{hr-L}) for each disaster event and date and the time of occur-
rence are shown

Nosrati et al. 2011; Seiler et al. 2002) where both short-
and long-term flood events can be monitored as a single
time series index. A number of studies advocated the use
of an hourly index for temporal analysis of floods to
provide better insight into extreme rainfall behaviors
and effective representations of flood risk (Fujibe
1988; Sato and Takahashi 2000; Sen Roy 2009;
Winkler et al. 1988). In this study, the advantage of an

Table 5 Flood events recorded in Dobong Observatory (South Korea) from 1998 to 2013 ranked by monthly precipitation (P_{tot})

Rank	Year	Month	P_{tot}	WRI_{hr-L}	$WRI_{24-hr-S}$	$WRI_{48-hr-S}$	$WRI_{72-hr-S}$
1	1998	August	1062	539,188	6889	11,751	16,213
2	2006	July	1060	359,063	6738	11,476	15,875
3	2011	July	789	347,187	4879	8269	11,639
4	2013	July	753	275,898	4785	8068	11,059
5	2000	August	728	239,812	4548	7637	10,475
6	2001	July	701	201,815	4434	7491	10,303
7	2003	August	695	373,271	4417	7471	10,256
8	1999	August	653	395,832	4322	7476	10,385
9	2002	August	609	302,043	3747	6277	8591
10	2009	July	585	255,217	3718	6301	8699

The worst flood month is in italic. All units are in millimeters (mm)

WRI_{hr-L} long-term hourly Water Resources Index, $WRI_{24-hr-S}$ 24
hourly Water Resources Index, $WRI_{48-hr-S}$ 48 hourly Water Re-
sources Index, $WRI_{72-hr-S}$ 72 hourly Water Resources Index

hourly method was that it provided a universal frame-
work for analysis of changes in water resources on
various timescales (hourly, daily, monthly, annual) with-
in the context of a unified index for assessing large-scale
flood possibility (i.e., WRI_{hr-L}) and short-term rapid
events such as flash floods (WRI_{hr-S}). Consequently,
the water resources metric measured flood progression
based on short-term summations with accumulated rain-
fall ($D = 24, 48, 72, \text{etc.}$, hourly), as well as long-term
summation periods (365 or more days).

It should be acknowledged that in its current form,
the method makes a basic assumption that hourly rain-
fall accumulation over a 24-h period is expected to
redistribute following a linear function (Eq. 5). The
linear form emanates from the physical principle that
available water resources on a given day remain consis-
tent with earlier daily models (Eqs. 1–4) with an expo-
nentially decaying form of water resources to allow
consistency with stochastic rainfall runoff equations
(Byun and Jung 1998; Byun and Lee 2002; Choi et al.
2012; Deo et al. 2015; Fitzgerald 2007; Jonsdottir et al.
2006). Accordingly, a linear representation of
redistributed rainfall was established (Fig. 3b) where
the exponential form of the depletion of water resources
over a daily time step remained valid (Eqs. 1–4; Eqs. 6
and 7). It is important to mention that the exponential
decay of water volume was consistent with exponential
forms used in stochastic rainfall runoff models (Byun

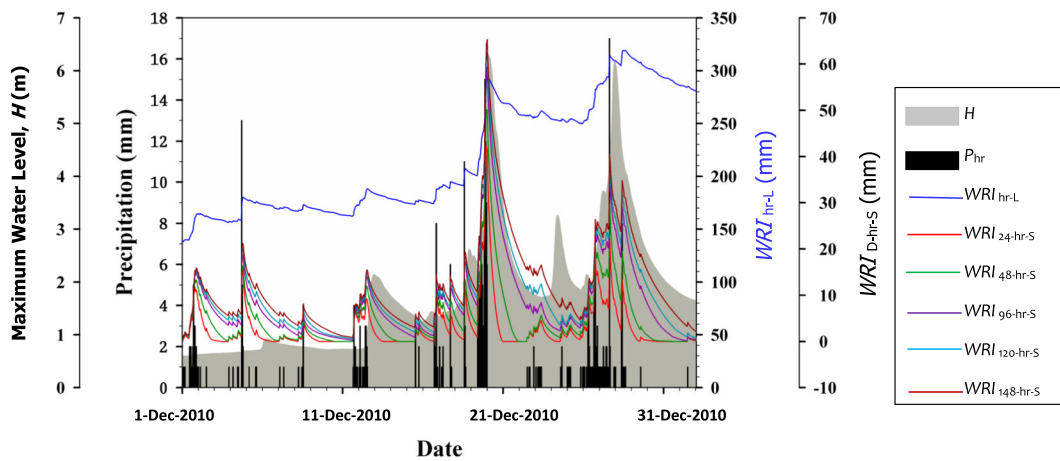


Fig. 12 Changes in the hourly long-term (WRI_{hr-L}) and the short-term water resources index (WRI_{D-hr-S}) in the severe flood event for the Brisbane River site (at Linville, Australia) with different

summation periods ($D = 24, 48, 96, 120,$ and 128 h). The precipitation and river water levels for each hour are also shown

and Jung 1998; Jonsdottir et al. 2006), soil moisture changes (Yamaguchi and Shinoda 2002), and daily flood progression analysis (Deo et al. 2015; Lu 2009).

Our work has utilized the negative exponential loss equation for quantifying the remaining water volume, similar to studies that described water deficits or abundance due to precipitation changes (Chen et al. 2015; Lu 2009; Lu et al. 2015; Martin-Vide 2004). While embracing the relevance of these methods in their own right, a comparison of hourly, daily, monthly, and annual flood extent in the proposed water resources index merely depends on the choice of the weighing factor over the prescribed time step, thus showing its versatility and consistency with the other approaches.

In future research, particularly in different hydrological and topographic conditions, one should consider an exhaustive comparison of current formulae with rainfall runoff equations in hydrodynamic models and other forms of time-dependent reduction functions (other than the linear formulation for hourly and exponential formulation for daily time steps). In addition, for regions with different decay rates of the rainfall-accumulated water volumes, it will be important to incorporate the decay rates depending on the particular physiographic factors when developing the hourly flood risk index.

Conclusion

A novel hourly water resources index (WRI_{24-hr}) was developed, and its suitability for continuous monitoring

of flood risk was tested for two sites in South Korea (August 1998, Dobong Observatory) and Australia (December 2010–January 2011, Brisbane). $WRIs$ were found to be versatile flood indicators based on the physical principle that the risk can be judged by the current as well as the antecedent rainfall accumulation, where the contributions of antecedent rainfall into water resources decay over time due to physical factors (e.g., runoff, evapotranspiration, percolation). Two alternative forms of $WRIs$ were proposed: the short-term water resources index ($WRI_{24-hr-S}$), where rainfall accumulation for the most recent 24 h (i.e., P_{hr} measured at every hour) are analyzed for the short-term flood risk, and the long-term water resources index (WRI_{hr-L}), where the precipitation cycle (over the 365 days of hydrological period) is used to assess large-scale flooding situations. $WRIs$ were applied over hourly, daily and annual time steps to demonstrate their comprehensive applications on rainfall durations and amounts for flood risk monitoring. Variation of $WRI_{24-hr-S}$ was closely in-phase with hourly precipitation (thus reflecting the danger of flash flooding) and WRI_{hr-L} agreed well with mean water levels in nearby river systems. The latter metric was found to be a good indicator of large-scale flooding and was consistent with large-scale evacuation warnings within the vicinity of the Dobong Observatory.

Based on the results, there are several advantages of WRI . Firstly, in comparison with rainfall–runoff models that are complex in their development and require physical assumptions and parametric equations to analyze or monitor the risk, $WRIs$ are easy to compute, analyze, and

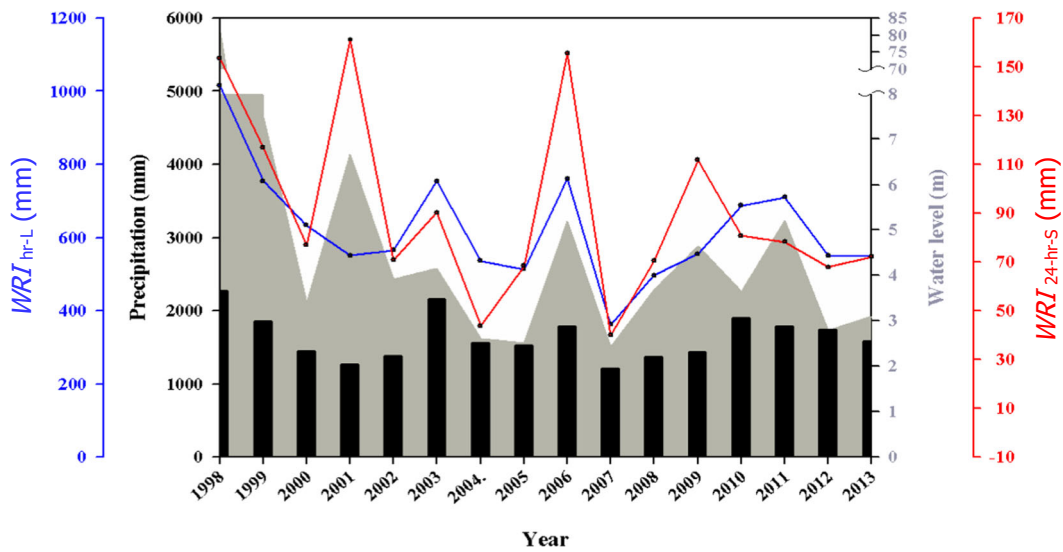


Fig. 13 Annual flood events identified for Dobong Observatory (South Korea) using the annual maximum value of the long-term (WRI_{hr-L}) and the short-term water resources index ($WRI_{24-hr-S}$) compared with the maximum precipitation and river water levels

physically interpret for a non-technical audience, as they utilize only precipitation data with less mathematical complexity and parametric-based assumptions. Secondly, $WRIs$ can potentially be used to advise infrastructural maintenance works if a certain threshold of the WRI was deemed insufficient for the site to withstand previously quantified water-related disasters. Consequently, the revised thresholds of WRI could be deduced, to counteract the vulnerability to future water-related disasters. For instance, consider the Jungryang Stream levee (Table 3) that could have been subjected to maintenance work after the August 1998 flood. However, in 2008 an inundation occurred again (MBC 2008), only with $WRI_{hr-L} = 498$ mm (Fig. 13). Although a causal factor for the inundation could be the different distribution of rainfall in the latter episode, one may also suspect that previous maintenance work was perhaps ineffective and thus required further attention by maintenance authorities. However, further work is needed before such connections between water disasters can be determined. Thirdly, $WRIs$ may be analyzed for ranking chains of heavy rainfall disasters, which would require modeling of disasters and trigger thresholds of the WRI . Subsequently, the statistical metric could also provide empirical flood monitoring data for modeling the potential likelihood of future disasters for a location. $WRIs$ can therefore be objective tools for assessing real-time effects of heavy rain events and their subsequent chain of disasters.

It should be noted that the time-evolution of $WRIs$ was useful in “predicting” water-related disasters.

However, $WRIs$ have limitations in generalizing their application to water-related disasters in geographically diverse sites, where the time reduction function needs to be reformulated to incorporate the role of physical factors. An accurate documentation of disasters and hourly rainfall is required before its implementation for wider usage, which is a difficult task for data-sparse sites, since records of disasters at many stations are neither documented clearly nor precisely enough. Fortunately, it is possible for meteorologists to restore these kinds of data if they have been archived. Another challenge is the verification of $WRIs$ for their broader applicability for interlinking index-based warnings with disaster. However, the success of the application provides an exploratory platform for scientists to test the index in other regions, provided documented records of disasters and hourly rainfall data can be established. The method can also be of assistance for flood mitigation as an adaptive paradigm for flood risk to reduce damage caused by rainfall events, to assist in the development of warnings for the public on the likelihood of disasters, and to reduce vulnerability by incorporating maintenance works on riverbanks and other infrastructure.

Acknowledgments We thank the reviewers and the Editor-in-Chief whose constructive comments have improved the clarity of the manuscript.

Funding information The research was supported by the Science Research Program through the National Research Foundation of Korea (NRF), funded by the Ministry of Education (No.

2013R1A1A4A01007626), Professor H. R. Byun; Australian Government Endeavour Fellowship program (No. 4293_2015) and Academic Division Researcher Activation Incentive Scheme (RAIS; July–September 2015), Dr. R.C. Deo; and an NSERC Discovery Grant, Professor J. F. Adamowski (McGill University, Canada).

References

- An, G., & Kim, J. (1998). A study on the simulation of runoff hydrograph by using artificial neural network. *Journal of Korea Water Resources Association* (In Korean), *31*, 13–25.
- Arnaud, P., Fine, J., & Lavabre, J. (2007). An hourly rainfall generation model applicable to all types of climate. *Atmospheric Research*, *85*(2), 230–242.
- Babister, M., Retallick, M. (2011) *Brisbane River 2011 flood event—flood frequency analysis*. Final Report. WMA water. Submission to Queensland Flood Commission of Inquiry.
- Badrzadeh, H., Sarukkalige, R., & Jayawardena, A. (2015). Hourly runoff forecasting for flood risk management: application of various computational intelligence models. *Journal of Hydrology*, *529*, 1633–1643.
- Beck, F., et al. (2015). Statistical analysis of sub-daily precipitation extremes in Singapore. *Journal of Hydrology: Regional Studies*, *3*, 337–358.
- BOM. (2012). *Inquiry into flood mitigation infrastructure in Victoria*. Melbourne: Bureau of Meteorology.
- Box, P., Thomalla, F., & Van Den Honert, R. (2013). Flood risk in Australia: whose responsibility is it, anyway? *Water*, *5*(4), 1580–1597.
- BTRE. (2002). *Benefits of flood mitigation in Australia*. Canberra: Bureau of Transport and Regional Economics, BTRE.
- Burnash, R., Singh, V. (1995) The NWS river forecast system-catchment modeling. *Computer models of watershed hydrology* (pp. 311–366).
- Byun, H.-R., & Jung, J. (1998). Quantified diagnosis of flood possibility by using effective precipitation index. *Journal of Korea Water Resources Association*, *31*(6), 657–665.
- Byun, H.-R., & Lee, D.-K. (2002). Defining three rainy seasons and the hydrological summer monsoon in Korea using available water resources index. *Journal of the Meteorological Society of Japan*, *80*(1), 33–44.
- Byun, H.-R., & Wilhite, D. A. (1999). Objective quantification of drought severity and duration. *Journal of Climate*, *12*(9), 2747–2756.
- Chen, W., Chen, C., Li, L., Xing, L., Huang, G., & Wu, C. (2015). Spatiotemporal analysis of extreme hourly precipitation patterns in Hainan Island, South China. *Water*, *7*(5), 2239–2253.
- Choi, K.-S., Wang, B., & Kim, D.-W. (2012). Changma onset definition in Korea using the available water resources index and its relation to the Antarctic oscillation. *Climate Dynamics*, *38*(3–4), 547–562.
- Crompton, R., 2011. Normalising the Insurance Council of Australia Natural Disaster Event List: 1967–2011. Report prepared for the Insurance Council of Australia, Risk Frontiers. <http://www.insurancecouncil.com.au/assets/files/normalising%20the%20insurance%20council%20of%20australia%20natural%20disaster%20event%20list.pdf>
- Dee, D., et al. (2011). The ERA-Interim reanalysis: configuration and performance of the data assimilation system. *Quarterly Journal of the Royal Meteorological Society*, *137*(656), 553–597.
- Deo, R. C., Byun, H.-R., Adamowski, J. F., & Kim, D.-W. (2015). A real-time flood monitoring index based on daily effective precipitation and its application to Brisbane and Lockyer Valley flood events. *Water Resources Management*, *29*(11), 4075–4409.
- Deo, R. C., Kisi, O., & Singh, V. P. (2017). Drought forecasting in eastern Australia using multivariate adaptive regression spline, least square support vector machine and M5Tree model. *Atmospheric Research*, *184*, 149–175.
- DNRM. (2014). *Establishing a new water monitoring site (WM65). Version 1.0*. Brisbane: State of Queensland (Department of Natural Resources and Mines), Service Delivery.
- Dogan, S., Berktaş, A., & Singh, V. P. (2012). Comparison of multi-monthly rainfall-based drought severity indices, with application to semi-arid Konya closed basin, Turkey. *Journal of Hydrology*, *470*, 255–268.
- Doswell, C. A., Brooks, H. E., & Maddox, R. A. (1996). Flash flood forecasting: an ingredients-based methodology. *Weather and Forecasting*, *11*(4), 560–581.
- Du, J., Fang, J., Xu, W., & Shi, P. (2013). Analysis of dry/wet conditions using the standardized precipitation index and its potential usefulness for drought/flood monitoring in Hunan Province, China. *Stochastic Environmental Research and Risk Assessment*, *27*(2), 377–387.
- Econopoulou, T., Davis, D., & Woolhiser, D. (1990). Parameter transferability for a daily rainfall disaggregation model. *Journal of Hydrology*, *118*(1), 209–228.
- Fitzgerald, D. (2007) Estimation of point rainfall frequencies. Irish Meteorological Service, Technical Note # 61, Glasnevin Hill, Dublin 9, Ireland.
- Fujibe, F. (1988). Weekday-weekend differences of urban climates. III: temperature and wind fields around Tokyo and Osaka. *Journal of the Meteorological Society of Japan*, *66*(2), 377–385.
- Gaal, L., Molnar, P., & Szolgay, J. (2014). Selection of intense rainfall events based on intensity thresholds and lightning data in Switzerland. *Hydrology and Earth System Sciences*, *18*(5), 1561–1573.
- Georgakakos, K. P. (2006). Analytical results for operational flash flood guidance. *Journal of Hydrology*, *317*(1), 81–103.
- Ghosh, S. et al. (2015) High resolution mapping of flood hazard for South Korea. EGU General Assembly Conference Abstracts, p. 1736.
- Glade, T. (1998). Establishing the frequency and magnitude of landslide-triggering rainstorm events in New Zealand. *Environmental Geology*, *35*(2–3), 160–174.
- Godt, J. W., Baum, R. L., & Chleborad, A. F. (2006). Rainfall characteristics for shallow landsliding in Seattle, Washington,

- USA. *Earth Surface Processes and Landforms*, 31(1), 97–110.
- Han, S. U., & Byun, H. R. (2006). The existence and the climatological characteristics of the spring rainy period in Korea. *International Journal of Climatology*, 26(5), 637–654.
- Helloco, F., Vidal, J.-J., & Chèze, J.-L. (2003). *GISELE: a new capability for flash flood early warnings over Garonne River sub-basins. Early warning systems for natural disaster Reduction* (pp. 277–282). Berlin: Springer.
- Hill, C., Verjee, F., Barrett, C. (2010) *Flash flood early warning system reference guide*. University Corporation for Atmospheric Research, ISBN. 978-970.
- HRFCO. (2014) Han River flood control office: water level on Jungryang Stream. Flood Control Office: <http://www.hrcco.go.kr/html/main/main.jsp>, South Korea.
- Inquiry, Q.F.C.o. (2011) Queensland Foods Commission of Inquiry: Interim Report, 1180 pp. Brisbane, Queensland, Australia., pp 1180 pp.
- IPCC. (2001) The scientific basis. Contribution of Working Group I to the Third Assessment Report of the Intergovernmental Panel on Climate Change. In: Houghton, J.T., Ding, Y., Griggs, D. J., Noguer, M., Van der Linden, P. J., Dai, X., Maskell, K. and Johnson, C. A. (eds.), Cambridge and New York: Cambridge University Press.
- Jakeman, A., & Homberger, G. (1993). How much complexity is warranted in a rainfall-runoff model? *Water Resources Research*, 29(8), 2637–2649.
- Jayasuriya, D. et al. (2011). Streamflow and water availability forecasts—exploring the needs of water managers and the community. In: E. E. A. C. J. Valentine, J. Ball, H. Chanson, R. Cox, R. Ettema, G. Kuczera, M. Lambert, B. W. Melville, J. E. Sargison (eds.). *Proceedings of the 34th World Congress of the International Association for Hydro- Environment Research and Engineering: 33rd Hydrology and Water Resources Symposium and 10th Conference on Hydraulics in Water Engineering* (pp. 782–789). Barton, A.C.T.: Engineers Australia. Availability: <http://search.informit.com.au/documentSummary;dn=321917139851808;res=IELENG>.
- Jonsdottir, H., Madsen, H., & Palsson, O. P. (2006). Parameter estimation in stochastic rainfall-runoff models. *Journal of Hydrology*, 326(1), 379–393.
- Keogh, D. U., Apan, A., Mushtaq, S., King, D., & Thomas, M. (2011). Resilience, vulnerability and adaptive capacity of an inland rural town prone to flooding: a climate change adaptation case study of Charleville, Queensland, Australia. *Natural Hazards*, 59(2), 699–723.
- Khalik, M., Ouarda, T., Ondo, J.-C., Gachon, P., & Bobée, B. (2006). Frequency analysis of a sequence of dependent and/or non-stationary hydro-meteorological observations: a review. *Journal of Hydrology*, 329(3), 534–552.
- Khan, D. M. et al. (2014) Report on the different flood risk assessment strategies: WP4/D4.1 (Project Contract No: 244047). United Kingdom.
- Kim, D.-W., Byun, H.-R., & Choi, K.-S. (2009). Evaluation, modification, and application of the effective drought index to 200-year drought climatology of Seoul, Korea. *Journal of Hydrology*, 378, 1), 1–1),12.
- Kim, D.-W., Byun, H.-R., Choi, K.-S., & Oh, S.-B. (2011). A spatiotemporal analysis of historical droughts in Korea. *Journal of Applied Meteorology and Climatology*, 50(9), 1895–1912.
- Kim, C. J., Park, M. J., & Lee, J. H. (2014). Analysis of climate change impacts on the spatial and frequency patterns of drought using a potential drought hazard mapping approach. *International Journal of Climatology*, 34(1), 61–80.
- Kisi, O., & Cimen, M. (2011). A wavelet-support vector machine conjunction model for monthly streamflow forecasting. *Journal of Hydrology*, 399(1), 132–140.
- Labat, D. (2005). Recent advances in wavelet analyses: part 1. A review of concepts. *Journal of Hydrology*, 314(1), 275–288.
- Laurenson, E., Mein, R., Singh, V. (1995). RORB: hydrograph synthesis by runoff routing. *Computer models of watershed hydrology* (pp. 151–164).
- Lee, S. (1998). Flood simulation with the variation of runoff coefficient in tank model. *Journal of Korea Water Resources Association* (In Korean), 31, 3–12.
- Lee, K. T., & Huang, J.-K. (2013). Runoff simulation considering time-varying partial contributing area based on current precipitation index. *Journal of Hydrology*, 486, 443–454.
- Lee, J., Hur, S. (2000) A study on the flood Characteristics and improvement of Flood control Capability at Junrang-Stream Watershed in Seoul. *4th international Conference on Hydro-Science and -Engineering*, Water Resource Association, September 26–29, Seoul Korea.
- Liu, Y., Yang, X., Ren, L., Yuan, F., Jiang, S., & Ma, M. (2015). A new physically based self-calibrating Palmer Drought Severity Index and its performance evaluation. *Water Resources Management*, 29(13), 4833–4847.
- Lu, E. (2009) Determining the start, duration, and strength of flood and drought with daily precipitation: Rationale. *Geophysical Research Letters*, 36(12).
- Lu, E. (2012) Monitoring and maintenance of a cold-season drought. *Science and Technology Infusion Climate Bulletin NOAA's National Weather Service*, Fort Collins, CO (USA).
- Lu, E. et al. (2013) The day-to-day monitoring of the 2011 severe drought in China. *Climate Dynamics*, 1–9.
- Lu, E., Zhao, W., Gong, L., Chen, H., Wang, H., Li, X., Song, J., Tu, J., Higgins, R. W., & Halpert, M. S. (2015). Determining starting time and duration of extreme precipitation events based on intensity. *Climate Research*, 63(1), 31–41.
- Lumbroso, D., & Gaume, E. (2012). Reducing the uncertainty in indirect estimates of extreme flash flood discharges. *Journal of Hydrology*, 414, 16–30.
- Ma, T., Li, C., Lu, Z., & Wang, B. (2014). An effective antecedent precipitation model derived from the power-law relationship between landslide occurrence and rainfall level. *Geomorphology*, 216, 187–192.
- Mallat, S. G. (1989). A theory for multiresolution signal decomposition: the wavelet representation. Pattern analysis and machine intelligence. *IEEE Transactions*, 11(7), 674–693.
- Mallat, S. G. (1998). *A wavelet tour of signal processing*. New York: Academic.
- Martin-Vide, J. (2004). Spatial distribution of a daily precipitation concentration index in peninsular Spain. *International Journal of Climatology*, 24(8), 959–971.
- MBC. (2008). Moonwha Broadcasting Company. News July 24. (In Korean).
- MOLIT. (1999). Hydrological annual report in Korea 1998 by Ministry of Land, Infrastructure and Transport of Republic

- of Korea. Korean Government 42000-58720-56-10. 1180. (In Korean).
- MOLIT (2014) The enforcement regulation No. 23 for the law of river. Korean Government 42000-58720-56-10. 1180. (In Korean). <http://www.law.go.kr/LSW/lsInfoP.do?lsiSeq=112268#0000>.
- Moon, Y.-I., Kim, J.-S. (2015). General characteristics of causes of urban flood damage and flood forecasting/warning system in Seoul, Korea Young-II Moon¹, 2, Jong-Suk Kim¹, 2 1 Department of Civil Engineering, University of Seoul, Seoul 130–743, South Korea 2 Urban Flood Research Inst. EGU General Assembly Conference Abstracts, pp. 8193.
- NCC. (2011). *Frequent heavy rain events in late 2010/early 2011 lead to widespread flooding across Eastern Australia*. Melbourne: National Climate Centre, Special Climate Statement, Bureau of Meteorology.
- Nosrati, K., Saravi, M., & Shahbazi, A. (2011). Investigation of flood event possibility over Iran using the Flood Index. In H. Gökçekus, U. Türker, & J. W. LaMoreaux (Eds.), *Survival and sustainability: environmental concerns in the 21st century* (pp. 1355–1362). Iran: Springer.
- O'Brien, M. (2011) Brisbane flooding January 2011: An avoidable disaster. Submission in Response to Hydraulic Modelling Reports, 31 August 2011.
- Oh, K., Yu, I., Kim, H., Kim, S., Kim, L. H., & Jeong, S. (2015). Drought assessment based on real-time drought index. *Desalination and Water Treatment*, 53(11), 3111–3117.
- Park, D. (2006). One of the nowcasting applications: early warning systems for natural disasters in Korea. Oct, National Institute for Disaster Prevention, National Emergency Management Agency Seoul, Republic of Korea.
- Park, C.-K., Byun, H.-R., Deo, R. C., & Lee, B.-R. (2015a). Drought prediction till 2100 under RCP 8.5 climate change scenarios for Korea. *Journal of Hydrology*, 526, 221–230.
- Park, S.-R., Oh, S.-B., & Byun, H.-R. (2015b). Definition and characteristics of the water abundant season in Korea. *Theoretical and Applied Climatology*, 120(1–2), 249–258.
- Raupach, M. et al. (2009). Australian water availability project (AWAP): CSIRO marine and atmospheric research component: final report for phase 3. Melbourne: Centre for Australian Weather and Climate Research (Bureau of Meteorology and CSIRO), pp. 67.
- Ruiz-Villanueva, V., Borga, M., Zoccatelli, D., Marchi, L., Gaume, E., & Ehret, U. (2012). Extreme flood response to short-duration convective rainfall in South-West Germany. *Hydrology and Earth System Sciences*, 16(5), 1543–1559.
- Sassa, K., & Canuti, P. (2008). *Landslides—disaster risk reduction*. Berlin: Springer Science & Business Media.
- Sato, N., & Takahashi, M. (2000). Long-term changes in the properties of summer precipitation in the Tokyo area. *Tenki*, 47(9), 304–308.
- Seiler, R., Hayes, M. J., & Bressan, L. (2002). Using the standardized precipitation index for flood risk monitoring. *International Journal of Climatology*, 22(11), 1365–1376.
- Sen Roy, S. (2009). A spatial analysis of extreme hourly precipitation patterns in India. *International Journal of Climatology*, 29(3), 345–355.
- Seqwater. (2011). January 2011 flood event: report on the operation of Somerset Dam and Wivenhoe Dam *Review of Hydrological Issues* Queensland Government, Melbourne, Australia, 77pp.
- Toth, E., Brath, A., & Montanari, A. (2000). Comparison of short-term rainfall prediction models for real-time flood forecasting. *Journal of Hydrology*, 239(1), 132–147.
- van den Honert, R. C., & McAneney, J. (2011). The 2011 Brisbane floods: causes, impacts and implications. *Water*, 3(4), 1149–1173.
- Winkler, J. A., Skeeter, B. R., & Yamamoto, P. D. (1988). Seasonal variations in the diurnal characteristics of heavy hourly precipitation across the United States. *Monthly Weather Review*, 116(8), 1641–1658.
- Woolhiser, D., & Osborn, H. (1985). A stochastic model of dimensionless thunderstorm rainfall. *Water Resources Research*, 21(4), 511–522.
- Yamaguchi, Y., & Shinoda, M. (2002). Soil moisture modeling based on multiyear observations in the Sahel. *Journal of Applied Meteorology*, 41(11), 1140–1146.
- Yeo, S. W. (2002). Flooding in Australia: a review of events in 1998. *Natural Hazards*, 25(2), 177–191.
- Yonhapnews. (1998). Collected articles from Yonhapnews 04-09 Aug. (In Korean).
- Yonhapnews. (2004). Collected articles from Yonhapnews. July 16 (In Korean).
- Yu, F.-C., Chen, T.-C., Lin, M.-L., Chen, C.-Y., & Yu, W.-H. (2006). Landslides and rainfall characteristics analysis in Taipei City during the Typhoon Nari event. *Natural Hazards*, 37(1–2), 153–167.
- Zêzere, J., Trigo, R., Fragoso, M., Oliveira, S., & Garcia, R. (2008). Rainfall-triggered landslides in the Lisbon region over 2006 and relationships with the North Atlantic Oscillation. *Natural Hazards and Earth System Science*, 8(3), 483–499.
- Zhou, Y., Ma, Z., & Wang, L. (2002). Chaotic dynamics of the flood series in the Huaihe River Basin for the last 500 years. *Journal of Hydrology*, 258(1), 100–110.